PERGAMON

Journal of Structural Geology 22 (2000) 207–230

JOURNAL OF STRUCTURAL GEOLOGY

www.elsevier.nl/locate/jstrugeo

The control of the smectite–illite transition on passive-roof duplex formation: Canadian Rockies Foothills, Alberta

Brent A. Couzens-Schultz*, [1], David V. Wiltschko

The Center for Tectonophysics, Department of Geology and Geophysics, Texas A&M University, College Station, TX 77843-3113, USA

Received 7 October 1997; accepted 12 September 1999

Abstract

The roof décollement to the passive-roof duplex and triangle zone in the central Foothills, Rocky Mountain thrust belt is located within a sequence of siliciclastic sediments dominated by shale/mudstone. It is unclear why the décollement is found at a certain level in the stratigraphy, when the whole package appears to have similar lithilogical and hence mechanical properties. Investigation of the mineralogy of the mudstones reveals that the clay fraction preserves a smectite-to-illite transition, which formed during maximum burial conditions. The top of the transition is associated with the top of the roof décollement in the region. In the Gulf of Mexico, the transition correlates with both a zone of overpressure, favorable for detachment, and a corresponding drop in density (rise in porosity). In the Foothills, the transition also records a drop in density and a concomitant drop in sonic velocity. By analogy with the Gulf of Mexico, the drop in density may record a paleo-overpressured horizon that was favorable for detachment and formation of a roof décollement in the Foothills.

1. Introduction

Passive-roof duplexes, or triangle zones, are thought to form in deforming foreland basins that contain large amounts of shale. The shales are often part of a several-thousand-meter-thick, homogeneous siliciclastic section that is commonly synorogenic (Couzens and Wiltschko, 1996). As a thrust belt propagates into such a section, it forms thrust sheets at depth that generally consist of older, stronger rocks underlying the shale-rich basin, such as those of a carbonate platform, and a portion of the lower stratigraphy in the foreland basin. Somewhere, within the middle of the shale-rich section, a roof décollement forms above the thrust sheets, and the thrust sheets are thought to, at least in part, underthrust the upper portion of the shale-rich section.

The Foothills thrust belt in the Canadian Rockies contains a passive-roof duplex in such a shale-rich foreland basin. The triangle zone there forms in a 2000+-m-thick homogeneous sequence of upper Cretaceous and Tertiary shales, siltstones and sandstones, with the roof décollement located in the middle of the sequence (Fig. 1). Beneath the roof décollement, rocks are imbricated in thrust sheets, and above it they are passively bent up as a cover (Fig. 2). There is no clear lithological or strength difference between rocks in the upper bendable cover and those in the thrust sheets, yet there is a décollement between the two, and they behave very differently during deformation. The focus of this paper is to investigate why a décollement forms within the middle of such shale-rich sequences.

Given that the amount of sandstone within the horse blocks, roof décollement and cover are fairly similar, and that sandstones do not vary a great deal in strength, it seems reasonable to suspect that some property of the shale or mud/siltstone is responsible for the different deformation styles. The fine-grained nature of mudstone means that, although two rocks

* Corresponding author.
E-mail address: bcouz@shellus.com (B.A. Couzens-Schultz).
[1] Current address: Shell E&P Technology Applications and Research, P.O. Box 481, Houston, TX 77001, USA.

0191-8141/00/$ - see front matter
PII: S0191-8141(99)00151-0

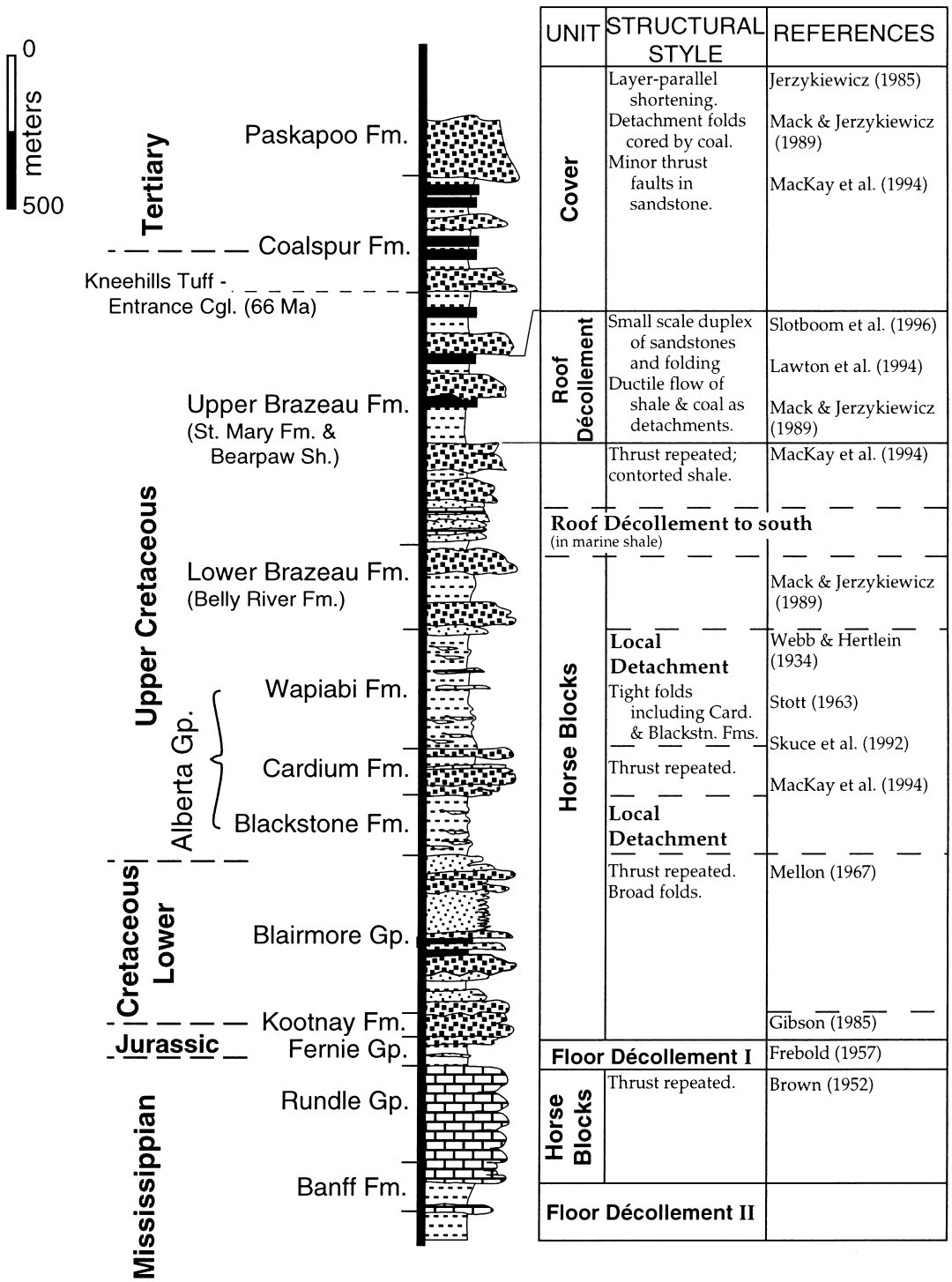

Fig. 1. Generalized stratigraphic column for the central Foothills thrust belt, Alberta.

may look identical in outcrop, they could have radically different compositions and strength properties (e.g. Clarke, 1966, pp. 268–269).

As a general working hypothesis, we propose that differences in the mineralogy of the mudstones caused either by differences in the original sediment or by burial diagenesis affect where the roof décollement forms in the basin. Depositional differences might include the amount of quartz within the mudstones compared to the amount of smectite. Quartz would make the mudstone relatively strong, whereas smectite would make it relatively weak. Burial diagenesis would mainly cause both the loss of porosity and the dewatering of clay minerals. The most important mineralogical change,

from smectite to illite, would increase the intrinsic strength of the rocks. The strength difference between smectite and illite is thought to be because the water interlayers create weak links between the sheets in the crystal structure (e.g. Wang and Mao, 1979; Wang et al., 1979; Shimamoto and Logan, 1981).

There is reason to believe that the smectite-to-illite (S–I) transition in clay mineralogy of shales is important in controlling the roof décollement location. Several authors have correlated the S–I transition in extensional regimes with either the location or attitude of normal faults (e.g. Burst, 1969; Evamy et al., 1978; Bruce, 1984, his fig. 9). For instance, Bruce (1984) and others show that normal faults flatten into and below the S–I transition zone and steepen above it. Also, in the Gulf Coast region, the S–I transition corresponds to either the top of the overpressured zone or a zone of steep fluid pressure gradient (e.g. Kerr and Barrington, 1961; Powers, 1967; Perry and Hower, 1972; Freed, 1982; Bruce, 1984; Pollastro, 1985). The mechanism for this increase in fluid pressure is thought to be both the release of the bound water from the smectite structure as it transforms to illite and a reduction in permeability due to the formation of mats of larger illite crystallites (Freed and Peacor, 1989a). Not only is new free water released to the pores, but water that is generated from the underlying compacting sediments cannot quickly escape upwards through the illite mats.

In compressional settings, Tribble (1990) and Wilkens et al. (1990) noted that the basal décollement of the Barbados accretionary prism is located at the base of the most smectite-rich part of the section. Vrolijk (1990) made a similar correlation at several subduction zones by compiling data on shale mineralogy from several sources. He noted that the aseismic–

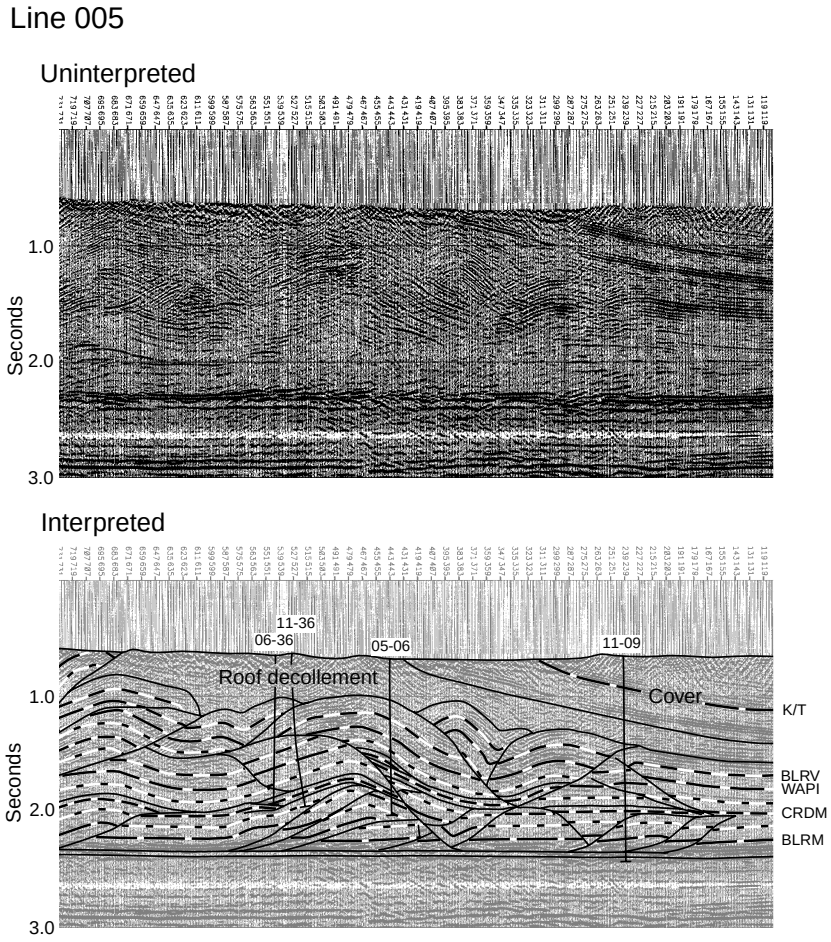

Fig. 2. Three representative seismic sections across the frontal monocline and triangle zone. Uninterpreted and interpreted sections are shown for each line. The seismic data are grayed in the interpreted sections. The lines are located approximately 6, 12 and 18 km north of the Red Deer River, near Sundre, AB. (a) Line 005. (b) Line 006. (c) Line 007. K/T — Cretaceous/Tertiary boundary, BLRV — top of the Belly River Formation = top of the lower Brazeau Formation, WAPI — top of the Wapiabi Formation, CRDM — Cardium Sandstone, BLRM — top of the Blairmore Group. Solid lines are thrust faults. Note that the upper Brazeau Formation and Tertiary sediments are passively uplifted in a monoclinal fold. These rocks are separated from thrust blocks in the lower section by a décollement zone in the upper Brazeau (Fig. 1).

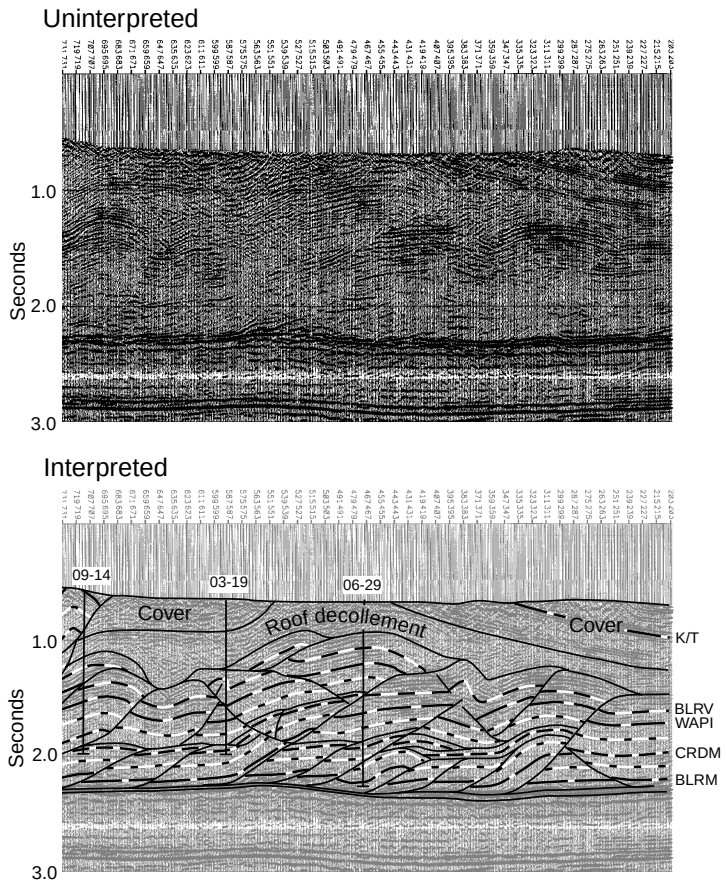

Fig. 2 (*continued*)

seismic transition also correlates with the S–I transition.

In the Foothills, the following observations support the S–I transition as a control on décollement location. The depth, and by inference temperature, at the time of deformation in the Foothills (Late Cretaceous–Paleocene) was in the range of temperature characteristic of the zone of rapid transformation from smectite to illite (50–145°C; Bruce, 1984; Freed and Peacor, 1989b). Coal moisture content (Nurkowski, 1985) and other data (Beaumont et al., 1985) support the conclusion that the depth of burial in the eastern Foothills was in the range of 2–3 km. Assuming a normal geothermal gradient, we would predict a temperature of 50–100°C at the top of the roof décollement during the maximum depth of burial. Although the transformation from smectite to illite is not instantaneous, it has been shown to be more temperature- than time-dependent (e.g. Bruce, 1984).

Because (i) the S–I transition is an important control on mechanical boundaries, and (ii) the Foothills foreland basin was at depths and temperatures reasonable for the S–I transition, we chose to examine the hypothesis that the location of the roof décollement of the Canadian Foothills passive-roof duplex is a result of changes in clay mineralogy in the upper Cretaceous mudstone units. We will specifically investigate the possibility that the changes are related to the S–I transition and subsequent formation of an overpressured zone within the shale basin.

To this end, 62 samples were collected from mudstone units within the cover, roof décollement, and horse blocks of the duplex (Fig. 3). Twenty-two of the samples are from four outcrops, and are used to determine the amount of local variability within the section. All of the samples were analyzed using powder X-ray diffraction to determine their mineralogy. Because our purpose is to make a correlation between the S–I transition and décollement location, we only examined the clay-sized fraction of the samples, where the transition is recorded. To further establish the possible existence of an overpressured zone related to burial diagenesis,

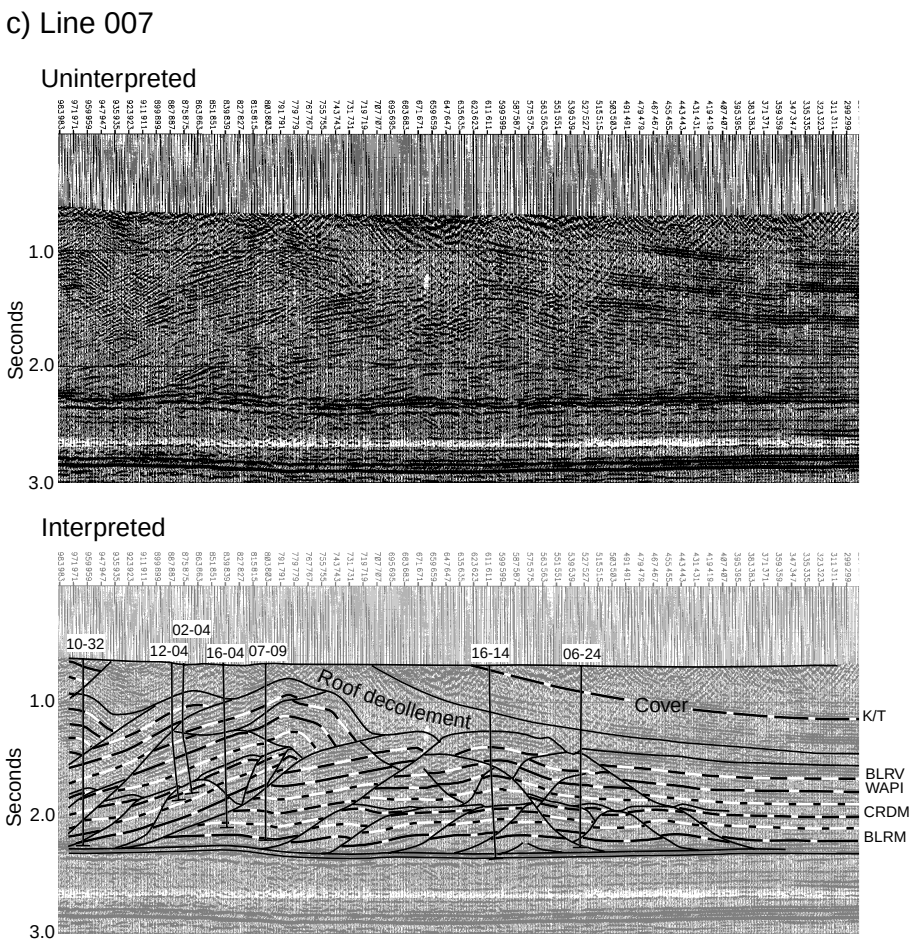

Fig. 2 (*continued*)

velocity and density data across the roof décollement were also investigated for comparison with known trends across the Gulf of Mexico S–I transition.

2. Regional geology

2.1. Stratigraphy sampled

The oldest units sampled are found entirely within the thrust sheets of the Foothills belt. They include marine shales from the Alberta Group which contains the basal Blackstone Formation, overlain by sandstones of the Cardium Formation and shales of the Wapiabi Formation (Fig. 1).

Above the Alberta Group, the stratigraphic nomenclature changes from north to south in the study area. In the central Foothills, north of the Bow River are rocks of the Brazeau Formation (Fig. 3). These rocks are entirely non-marine and consist of four cyclothems (Jerzykiewicz, 1985), each with a lower unit of thick channel sandstone layers and an upper unit of overbank deposits. The sandstones contain large proportions of volcanic rock fragments (30–50%) and plagioclase grains (25–35%) as well as mono- and polycrystalline quartz and chert grains. Carbonate sand grains are rare (< 1% in general; Mack and Jerzykiewicz, 1989). The Brazeau Formation is divided into an upper and lower member, with the base of the upper member corresponding roughly to the base of a lacustrine facies. To the south of the Bow River (Fig. 3), the upper Brazeau Formation correlates to the St. Mary River Formation and Bearpaw Shale, which grades into the lacustrine facies. The lower Brazeau correlates to the Belly River Formation (Mack and Jerzykiewicz, 1989). The southern equivalents were also deposited in mainly continental fluvial environments, with the exception of marginal marine facies at the base of the Belly River Formation and the marine Bearpaw Shale. The percentage of volcanic rock fragments and plagioclase grains in the sandstone layers of these formations is significantly less than in the Brazeau Formation (10–20% and 15–30% respectively; Mack and Jerzykiewicz, 1989).

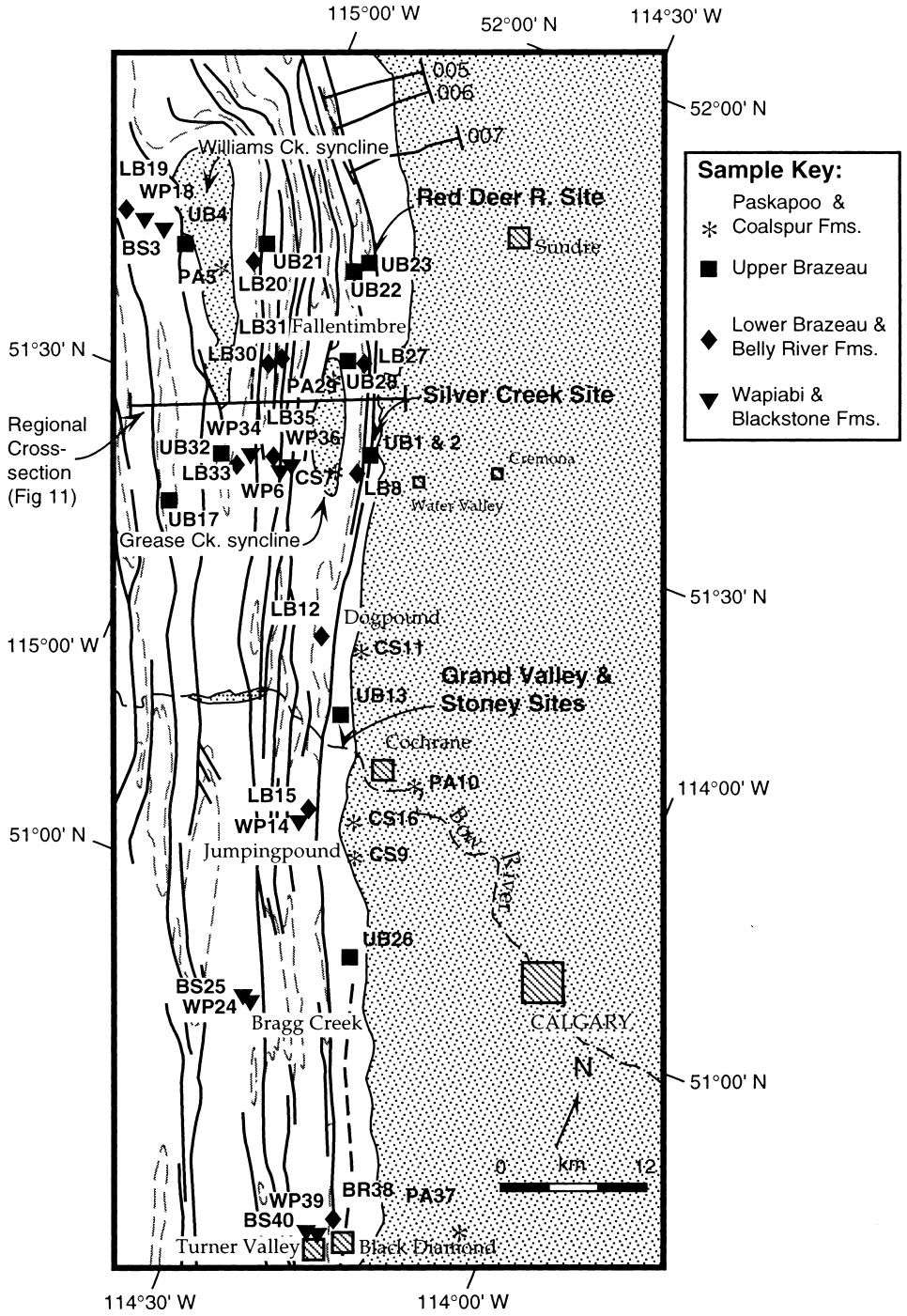

Fig. 3. Geology of the study area (after Ollerenshaw, 1965, 1969, 1972, 1974, 1975,1978; McMechan, 1995) showing locations of shale/mudstone samples, individually studied outcrops, a regional cross-section, and seismic lines shown in Fig. 2. Gray shaded regions are Tertiary rock units. White area indicates rocks within the thrust sheets (Brazeau Formation and Alberta Group). Dashed lines are the upper/lower Brazeau Fm. contacts. Thick solid lines are thrust faults.

Above the Brazeau Formation are uppermost Cretaceous and Tertiary rocks (Fig. 1). Formation names for the Tertiary stratigraphy vary in the literature. We follow the nomenclature of Mack and Jerzykiewicz (1989). In their system, the Kneehills tuff (dated at 66 Ma) corresponds to the base of the Coalspur Formation, with the Cretaceous/Tertiary boundary being contained within the Coalspur Formation (Fig. 1). The Coalspur Formation is a fifth cyclothem above the four in the Brazeau Formation

(Jerzykiewicz, 1985). About 350–400 m above the Coalspur Formation is the Paskapoo Formation (Fig. 1).

Carrigy (1971) broke the post-Kneehills strata into two facies: the volcanic rock fragment facies, and the clastic carbonate sandstone facies. North of the Bow River (Fig. 3), he saw that sandstones directly above the Kneehills tuff (the Coalspur Formation) contained mainly volcanic rock fragments. Above this, he saw an influx of carbonate clasts into the sandstones. Mack and Jerzykiewicz (1989) saw similar relationships and placed sandstones with the carbonate clasts in the Paskapoo Formation. To the south, Carrigy (1971) notes that both facies overlap above the Kneehills tuff. Therefore, the carbonate clasts are no longer a distinguishing feature of the Paskapoo Formation south of the Bow River. Mack and Jerzykiewicz (1989) report the same observation, and they see considerably fewer volcanic rock fragments overall.

2.2. Generalized structure

The frontal Foothills thrust belt involves Mississippian carbonates at depth and Cretaceous and Tertiary siliciclastics at the surface. Roughly, from the Bow River south (Fig. 3), the thrust-repeated portion of the frontal duplex involves Mississippian carbonates through upper Cretaceous siliciclastics (e.g. Shaw, 1963; Bally et al., 1966; Slotboom et al., 1996; MacKay, 1996). North of the Bow River, however, the carbonates are not always imbricated, but instead may underlie the floor thrust of the duplex (e.g. Soule and Spratt, 1996; see Fig. 2). They are incorporated into the Foothills thrust belt further towards the hinterland, as the floor detachment steps down to a deeper level (e.g. Bally et al., 1966; Dechesne and Muraro, 1996). Both north and south of the Bow River, the thrust repeated section of the duplex is overlain by a cover of upper Cretaceous to Tertiary siliciclastics that are passively bent up above the duplex horse blocks (Figs. 1 and 2).

The cover is separated from the thrust-repeated horse blocks by a roof décollement in the upper Cretaceous upper Brazeau Formation. In most of the study area, the décollement is not a single surface. At the scale of a seismic section, it is a zone of rocks that accommodates the discordance between thrust structures below and gently bent units of the cover above (Fig. 2). The décollement has a measurable thickness on the seismic data from the Red Deer River (Figs. 2 and 3) southward to at least the Bow River (Lawton et al., 1994; Slotboom et al., 1996; Soule and Spratt, 1996). South of the Bow River, in the Turner Valley area (Fig. 3), the décollement is located in the marine Bearpaw Shale (see Fig. 1), and it does not have a seismically resolvable thickness (MacKay et al., 1994).

3. Clay sample preparation

Sample preparation for X-ray diffraction analysis of the clay mineralogy was carried out following the techniques of Jackson (1969). Samples were smeared onto thin section plates as a thin film to align the clay platelets. The clay films were step-scanned from 2°–32° 2θ (Cu $K\alpha$ radiation) in 0.02° intervals at a rate of 2° per minute. Samples were X-rayed after air drying and saturation with ethylene glycol. Comparison of the two diffraction profiles allows the determination of discrete illite, which is unaffected by glycolation, and indicates the presence of swelling clays.

Several possible methods exist to calculate the proportions of expandable interlayers. These include examining peak spacing (e.g. Hower, 1981), peak spacing and intensity (e.g. Srodon, 1980), and the ratio of the saddle-peak intensity for the smectite peak (e.g. Inoue et al., 1989). All of these methods produce a semi-quantitative determination of the proportions of expandable interlayers. Sources of variability in the results include crystallite size distribution, the degree of preferred orientation, and the presence of discrete illite. In our samples, discrete illite was present in almost every case (Columns D and E, Table 1), and other clay-sized minerals are also present (Column F, Table 1). The resultant variability introduces errors of $\pm$10–15% (Inoue et al., 1989). With near pure illite–smectite mixtures, a second set of peaks at higher diffraction angles can be used to reduce error associated with crystallite size (Srodon, 1980; Hower, 1981). However, for most mudstones, this is a difficult method to use because those peaks are very small and are often interfered with by other minerals in the assemblage. In most of our cases, the peaks were not clearly present and/or lacked a well-defined apex.

We chose to determine compositions by using the location of the $(001)_{10}/(002)_{17}$ and $(002)_{10}/(003)_{17}$ (8.5°–10.5° 2θ and 15.5°–17.8° 2θ, respectively) peaks (Hower, 1981). These peaks shift location with respect to the I/S ratio (see Hower, 1981, his tables 3.2 and 3.3). The peak locations are located in Column C of Table 1 and the resultant interpretation of percent expandable layers are in Column B. The ordering of the illite layers may be random or of the 'alleverdite-type', which has systematically alternating illite and smectite layers. The locations of the peaks noted above are relatively insensitive to the type of ordering (Hower, 1981). The 16.9 Å smectite peak (approx. 5° 2θ, see Column C, Table 1), however, does behave differently for random vs. ordered I/S. For randomly interstratified layers, the peak does not shift with the interspersing of illite layers, but its intensity decreases until it is a shoulder at 60% illite. For ordered I/S, the peak shifts as illite layers are added, but the shift is

Table 1
XRD results[a]

A Sample	B % Expandable Layers	C Peaks (2-theta)	D Other Illite (% Exp.)	E Peaks (2-theta)	F Others
Grand Valley Site					
GV1	80–90% R	low shoulders: 10.0, 15.6, 5.24	10% I/S	8.92, 17.86	K, C, Q
GV2	95%+ R	shoulders: 10.4, 15.76, 5.28	10% I/S	8.98, 17.80	K, Q
GV3	95%+ R	10.30, 15.74, 5.26	None		±K, Q
GV4	60–80% I/S	shoulders: 9.8–10.0, 15.6–16.0, 5.32	10% I/S	8.96, 17.86	K, C, Q
GV5	80–90% R	shoulders: 10.0–10.4, 15.5, 5.30	10% I/S	8.96, 17.88	K, C, Q
Stoney Site					
ST1	95%+ R	10.38, 15.80, 5.32	10–20% I/S	9.06, 17.70	K, Q
ST2	80–90% R	10.20, 15.94, 5.18	5% I/S	8.70, 17.84	K, C, Q
ST3	60% R	9.5–9.9, 16.2, 5.22	10–20% I/S	9.05, 16.8+	K, Q
ST4	95%+ R	shoulder: 10.3, 15.6, 5.14	10% I/S	8.98, 17.84	K, Q
ST5	90% R	10.1, 15.6, 5.24	10% I/S	8.92, 17.86	K, Q
ST6	30–40% I/S	9.38, 16.60, 5.36			K, Q
Silver Creek Site					
SC1	60% R	low shoulder: 9.8+, 16.2–16.7, 6.20, 5.26	10% I/S	8.94, 17.88	K, Q
SC2	80–90% R	shoulder: 10.2, 15.84, 5.24	10% I/S	8.96, 17.90	K, Q
SC3	80% R	shoulder: 10.0, 15.74, 5.32	20–30% I/S	9.20, 16.90	K, Q
SC4	50% R	shoulder: 9.50, 16.16, 6.22, 5.06	5% I/S	8.86, 17.80	K, C, Q
SC5	50–60% R	shoulder: 9.3, 16.58, 6.11 small shoulder: 4.80	10% I/S	8.96, 17.88	K, Q
SC6	60–80% R	shoulder: 9.5–10.0, 16.0, 5.22	10–15% I/S	9.00, 17.50	K, Q
SC7	Little S	5.36 (some minor S)	Little I	8.94	K, Q*
Red Deer River Site					
RD1	Little S		Little 15% I/S	~9.00	K, Q*
RD2	Little I/S	5.18 S, <10.0, >16.0			K, Q*
RD3	Little S	5.08 suggests some S			K, Q*
RD4	40–50% I/S	shoulders: 9.6–9.7, 16.5–16.7	10% I/S	8.90, 17.80	K, Q
Paskapoo & Coalspur Samples					
PA5	Little S	4.96 suggests some S	5% I/S	8.82, 17.74	K, Q
PA29	60% R	shoulders: <10.0, 16.0, 5.9, 5.18	5% I/S	8.82, 17.74	K, Q
PA10	40% I/S	shoulders: 9.50–10.0, 16.1, 6.1, 5.14	10% I/S	8.86, 17.76	K, C, Q
PA37	95%+ R	shoulder: 10.3–10.4, 15.7, 5.08	5% I/S	8.76, 17.68	K, Q
CS7	95%+ R	shoulder: 10.4, 15.78, 5.32	10% I/S	8.94, 17.86	K, Q
CS11	95%+ R	10.40, 15.75, 5.24	10% I/S	8.92, 17.82	K, C, Q
CS9	90% R	weak shoulder 9.5–10.5, 15.7 5.16 strong	5% I/S	8.84, 17.78	K, C, Q
CS16	95%+ R	shoulders 10.4, 15.7, 5.14	10% I/S	8.90, 17.78	K, Q
Upper Brazeau Samples					
UB1	90% R	9.8–10.2, 15.58, 5.14	Little I	8.86	K, Q
UB2	90% R	shoulder: 10.1, 15.75, 5.04	Little 5% I/S	8.72, 17.64	Q
UB13	95%+ R	10.30, 15.62, 5.08	Little I	8.84	K, Q
UB26	90% R	9.8–10.2, 15.6	Little 5% I/S	8.82, 17.74	K, ±Q
UB4	80% R	shoulder: 9.98–10.2, 15.72, 5.14	10% I/S	8.90, 17.80	K, Q, ±C
UB28	95%+ R	shoulder: 10.3, 15.8, 5.11	5% I/S	8.82, 17.72	K, Q
UB23	40–60% I/S	shoulders: 9.4–9.7, 16.3–16.7, 5.14	5% I/S	8.84, 17.76	K, ±Q
UB22	60–70% R	shoulders: 9.9–10.1, 16.0+, 5.14	Little 5% I/S	8.84	K, ±C, ±Q
UB21	40–50% I/S	shoulders: 9.5–9.9, 16.4–16.6, 5.20	Little 5% I/S	8.85	K
UB32	40–60% I/S	shoulders: 9.6–10.0, 16.1–16.4, 5.18	5% I/S	8.78, 17.80	K, Q
UB17	40–60% I/S	shoulders: 9.6, 16.1–16.4, 5.18	5% I/S	8.78, 17.70	K, Q
Belly River Sample					
BR38	95+%	10.36, 15.75, 5.02	5% I/S	8.77, 17.72	K, ±Q
Lower Brazeau Samples					
LB27	60–70% R	shoulders: 9.5–10.1, 15.8–16.3, 5.20	5% I/S	8.85, 17.80	K, ±Q
LB8	40–60% I/S	shoulders: 9.5–10.0, 16.2–16.7, 5.38	10% I/S	8.90, 17.86	K, Q
LB12	40% I/S	shoulders: 9.5, 16.75, 5.22	5% I/S	8.78, 17.70	K, Q
LB15	40–60% I/S	shoulders: 9.5–9.7, 16.0+, 5.06	5% I/S	8.70, 17.58	K, Q
LB31	60% R	shoulders: 9.5–10.1, 16.2–16.5, 5.18	5% I/S	8.80, 17.78	K, ±Q
LB30	40–60% I/S	shoulders: 9.4–9.6, 16.5+, 5.28	10% I/S	8.92, 17.74	K, ±Q

Table 1 (*continued*)

A Sample	B % Expandable Layers	C Peaks (2-theta)	D Other Illite (% Exp.)	E Peaks (2-theta)	F Others
LB35	40–60% I/S	shoulders: 9.5–10.1, 16.3+, 5.20	5% I/S	8.84, 17.88	K, Q
LB20	40–60% I/S	shoulders: 9.5+, 16.5–16.6, 5.10	5% I/S	8.82, 17.78	K
LB33	40–60% I/S	shoulders: 9.5+, 16.5, 5.18	Little 5% I/S	8.86	K, ±Q
LB19	Little S		5% I/S	8.80, 17.64	K, Q
Wapiabi Samples					
WP39	20–30% I/S	shoulders: 8.9–9.2, 16.6+, 6.60	10% I/S	8.89, 17.74	± K, ±Q
WP14	20–30% I/S	8.82, rise at 16.6+	5% I/S	8.82, 17.74	K, C, Q
WP36	30–40% I/S	shoulder: 9.3–9.6, 16.34, 5.28	10% I/S	8.98, 17.80	K, Q, ±C
WP6	40–50% I/S	shoulders: 9.4+, 16.3+, 5.48	5% I/S	8.88, 17.64	K, Q
WP34	Little S		5% I/S	8.82, 17.72	K, Q
WP24	40% I/S	shoulder: 9.3–9.5, 16.5, 5.28	5% I/S	8.82, 17.78	K, Q
WP18	20–30% I/S	8.84, rise at 16.6, 6.18	5% I/S	8.84, 17.76	K, Q
Blackstone Samples					
BS40	40% I/S	shoulder: 9.4–9.5, 16.4–17.0, 5.32	5% I/S	8.86, 17.74	K, ±Q
BS25	20–30% I/S	8.80, rise at 16.5, 6.20	5% I/S	8.80, 17.70	K, ±Q
BS3	20–30% I/S	8.78, shoulder: 16.7, 6.08	5% I/S	8.78, 17.68	K, Q

I/S — ordered illite/smectite, R — random illite/smectite, see text for determination of percent expandable layers. S — smectite, I — Illite, K — kaolinite, C — chlorite, Q — quartz, Q* — clay sized quartz is main constituent, ± — minor amounts present.

too sensitive to crystallite size and ordering to be useful for determining the proportion of illite layers.

4. Results

The results of powder X-ray diffraction analysis are summarized in Table 1. The individual X-ray diffraction patterns are shown in several figures that follow. These can be used for visual comparisons to validate the interpreted results found in Table 1. The samples are broken out by specific site locality, or by formation if only one sample was taken at a site. The mudstones contain quartz and kaolinite and discrete illite throughout the entire upper Cretaceous and Tertiary section (Table 1). The amount of smectite or mixed-layer illite–smectite clays varies most dramatically from sample to sample and therefore may be the cause of any strength differences among the mudstones.

First we will examine the samples from individual outcrop sites. These will be used to determine the variability that might be expected at any one sample site. Then we will examine the samples by formation and location within the structure of the thrust belt.

4.1. Individual outcrop sample sites

The Grand Valley and Stoney outcrop sites are located along the Bow River at the thrust belt front (Figs. 4 and 5). The outcrops at these sites are within the upper Brazeau Formation. They include a portion of the cover (Figs. 1 and 2) at the eastern edge of the Grand Valley site which has been tilted 30° to the east, and rocks within structures in the top portion of the décollement zone, which predominately verge westward, towards the hinterland (Figs. 4 and 5).

At both of these sites there is an interlayering of smectite-rich beds with beds of mixed-layer clays within single outcrops. In general, at the Grand Valley site there is a decrease in pure smectite from the cover towards the décollement zone. However, within the top of the décollement zone at the Stoney site, smectite-rich beds are found again. Also at the Stoney site, there is an appearance of beds with mixed-layer clays and a general decrease in expandable clay interlayers deeper into the décollement zone (Table 1).

The Silver Creek site consists of eight samples taken from the upper Brazeau Formation at the thrust front. Four of the samples (SC5, SC6, SC7 and UB2) are from the eastward dipping cover that is above the roof décollement (Fig. 6). These samples include a smectite-rich mudstone, a quartz-rich mudstone, and two mudstones that contain mixed-layer illite–smectite with 20–50% illite interlayers. There appears to be an increase in illite layer content down-section.

The other four samples at Silver Creek are from an anticlinal structure that is within the upper décollement zone and contains a backthrust with about 600 m displacement (Soule and Spratt, 1996). In the décollement zone, two beds have smectite with 10–20% random illite interlayers, and two beds have 40–50% illite interlayers in smectite (Table 1).

The Red Deer River site includes four samples from an outcrop beneath the roof décollement within the Brazeau thrust sheet (Fig. 7). These samples all contain quartz in the clay fraction and three of them are domi-

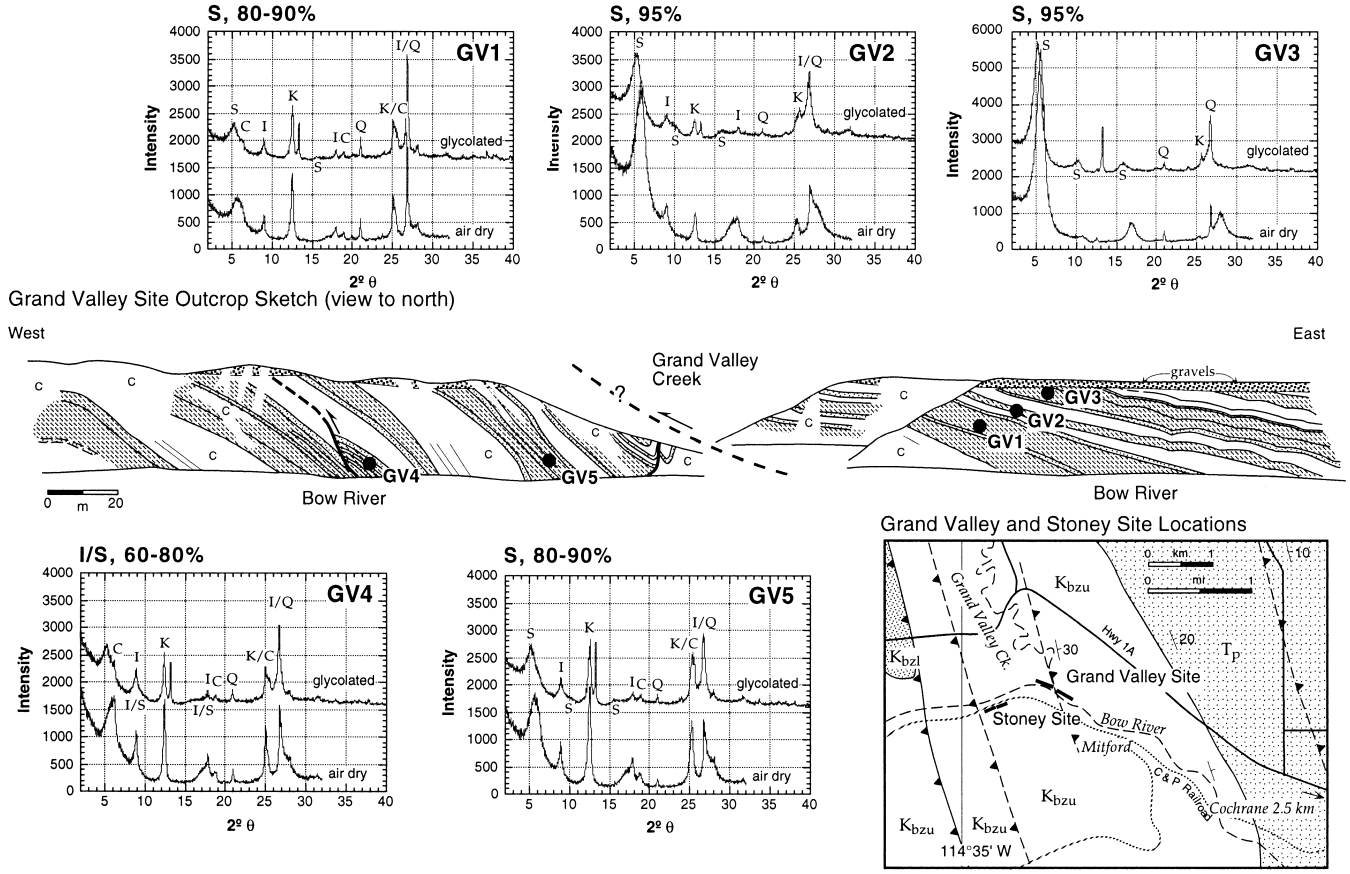

Fig. 4. Sketch of outcrop at the Grand Valley site showing the location of mudstone samples. Map shows the location of the outcrop (see Fig. 3 for map location). Tp — Tertiary, Kbzu — upper Brazeau Formation, Kbzl — lower Brazeau Formation. Graphs show the X-ray diffraction profiles for the clay fraction of each of the samples. Both the air dried and the glycolated profiles are shown for comparison. S — smectite, I — illite, I/S — mixed layer, K — kaolinite, C — chlorite, Q — quartz. Secondary peaks and shoulders for smectite and mixed-layer clays are labeled beneath the profile. Interpretation of the percentage of smectite interlayers is shown at the top-left of each plot.

nated by quartz. One sample (RD4) also contains mixed-layer illite–smectite with 50–60% illite interlayers (Table 1).

4.2. Coalspur and Paskapoo Formation mudstones

A rough estimate of stratigraphic height above the upper Brazeau contact at a sample location can be calculated using the dip of beds and map distance from the contact. This estimate was used to predict the location of the sample within the stratigraphy. Then, the petrology of the adjacent sandstones at the sample site was used to confirm location within either the Coalspur or Paskapoo Formations. North of the Bow River, sandstone clast composition is useful in assigning a sample site to either the Coalspur or Paskapoo Formation. This is because the Coalspur Formation is dominated by volcanic rock fragments whereas the Paskapoo Formation contains carbonate clasts (Carrigy, 1971; Mack and Jerzykiewicz, 1989). South of the Bow River both volcanic rock fragments and carbonate clasts are present in the sandstones of both formations, so the distinction is not useful.

Four samples were collected at 400+ m above the contact and are considered to be part of the Paskapoo Formation (Fig. 8). North of the Bow River, these sample were adjacent to sandstones containing carbonate clasts, confirming their location within part of the Paskapoo Formation (Fig. 9a). South of the Bow River, as predicted by Carrigy (1971), sample PA37 at Turner Valley is adjacent to sandstones with both carbonate clasts and volcanic rock fragments (Fig. 9c). Four other samples were collected from within 200 m above the upper Brazeau contact and are considered to be part of the Coalspur Formation. Two samples north of the Bow River (CS7, CS11) along with one sample just south of the Bow River (CS16) were adjacent to sandstones dominated by volcanic rock fragments, confirming their position in Coalspur Formation (Fig. 9b). The other sample from south of

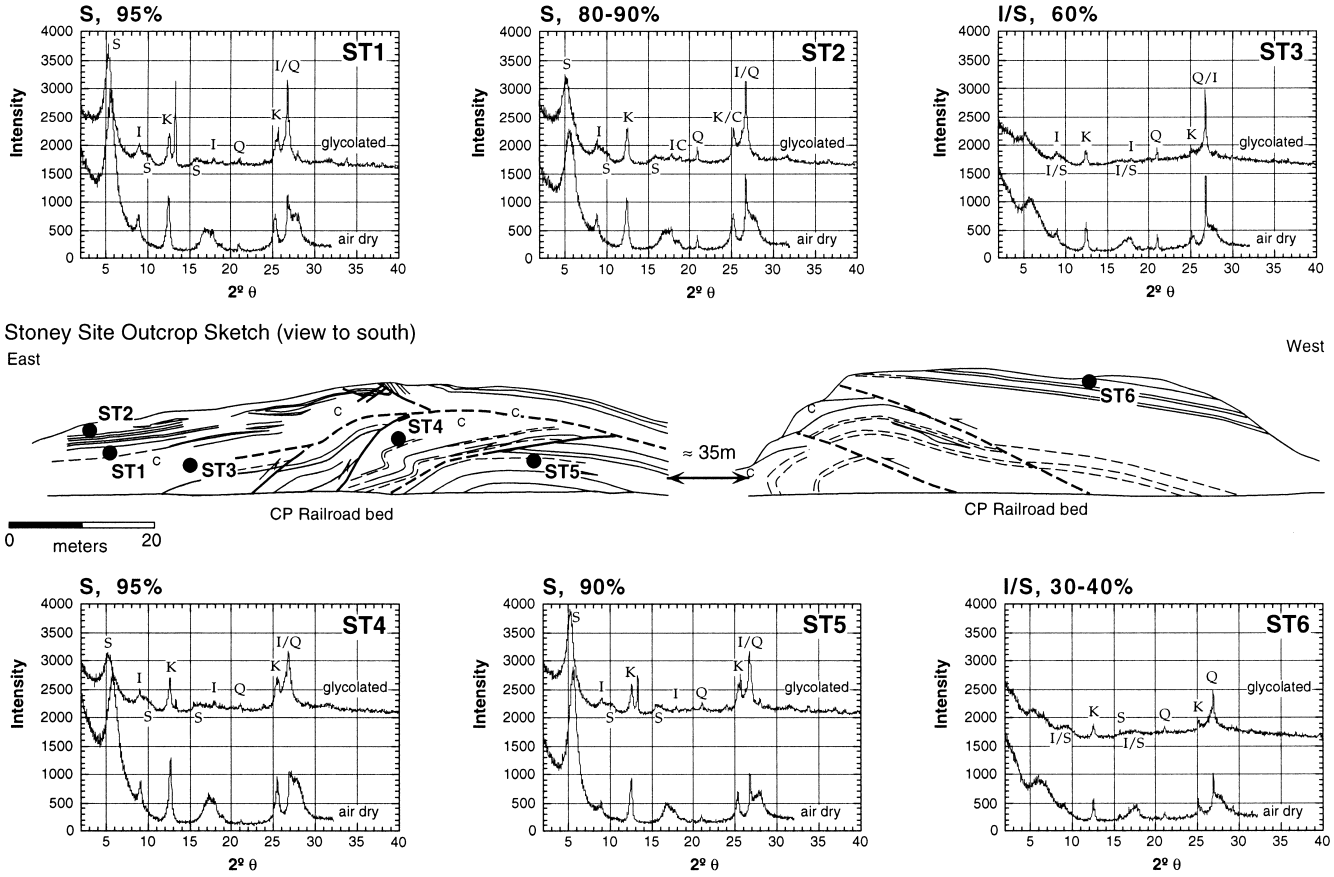

Fig. 5. Sketch of outcrop at Stoney site showing the location of mudstone samples. Map of outcrop location in Fig. 4. Graphs show the X-ray diffraction profiles for the clay fraction of each of the samples. Both the air dried and the glycolated profiles are shown for comparison. Symbols and labels as in Fig. 4. Interpretation of the percentage of smectite interlayers is shown at the top-left of each plot.

the Bow River (CS9) contains some carbonate clasts as well as volcanic rock fragments (Fig. 9c), as predicted by Carrigy (1971).

There is a distinct difference in mudstone clay mineralogy among the Tertiary samples (Fig. 8). North of the Bow River, mudstones from the Coalspur Formation largely contain smectite, whereas those from the Paskapoo Formation contain mixed-layer illite–smectite with 40–60% illite interlayers (Table 1). South of the Bow River, the mudstones from both formations contain some smectite, but peak intensities are much lower and there may be some mixed-layer illite–smectite as well.

4.3. Brazeau Formation mudstones

The mudstones of the upper Brazeau Formation fall into two distinct groups depending on their structural position. Samples structurally above and in front of the first emergent thrust, contain smectite that ranges from almost pure to about 20% illite interlayers (Fig. 10). These samples, including those at the Grand Valley, Stoney, and Silver Creek outcrops are all either from the cover or the upper portion of the roof décollement zone (Figs. 1 and 2). The individual outcrops demonstrate that although there are plenty of smectite-rich beds in this portion of the stratigraphy, there are also some smectite-poor beds.

Samples in the upper Brazeau Formation that are from within thrust sheets exposed in the Foothills contain mixed-layer illite–smectite with 40–60% illite interlayers (Fig. 10, Table 1). However, there are two exceptions. Samples UB4 and UB28 are within the thrust belt, apparently within thrust sheets, but contain smectite. These two samples are located near the Coalspur/Brazeau Formation contact in Tertiary synclines preserved within the thrust belt (Fig. 11). They are above the regional décollement level in the upper Brazeau and are therefore grouped with those samples in front of the thrust belt in the cover and roof décollement (Fig. 11)

Mudstones from the lower Brazeau Formation are all located within thrust sheets beneath the roof décollement (Figs. 11 and 12). The mudstones are reasonably consistent in their diffraction profiles (Fig. 12), and are interpreted to contain mainly mixed-layer

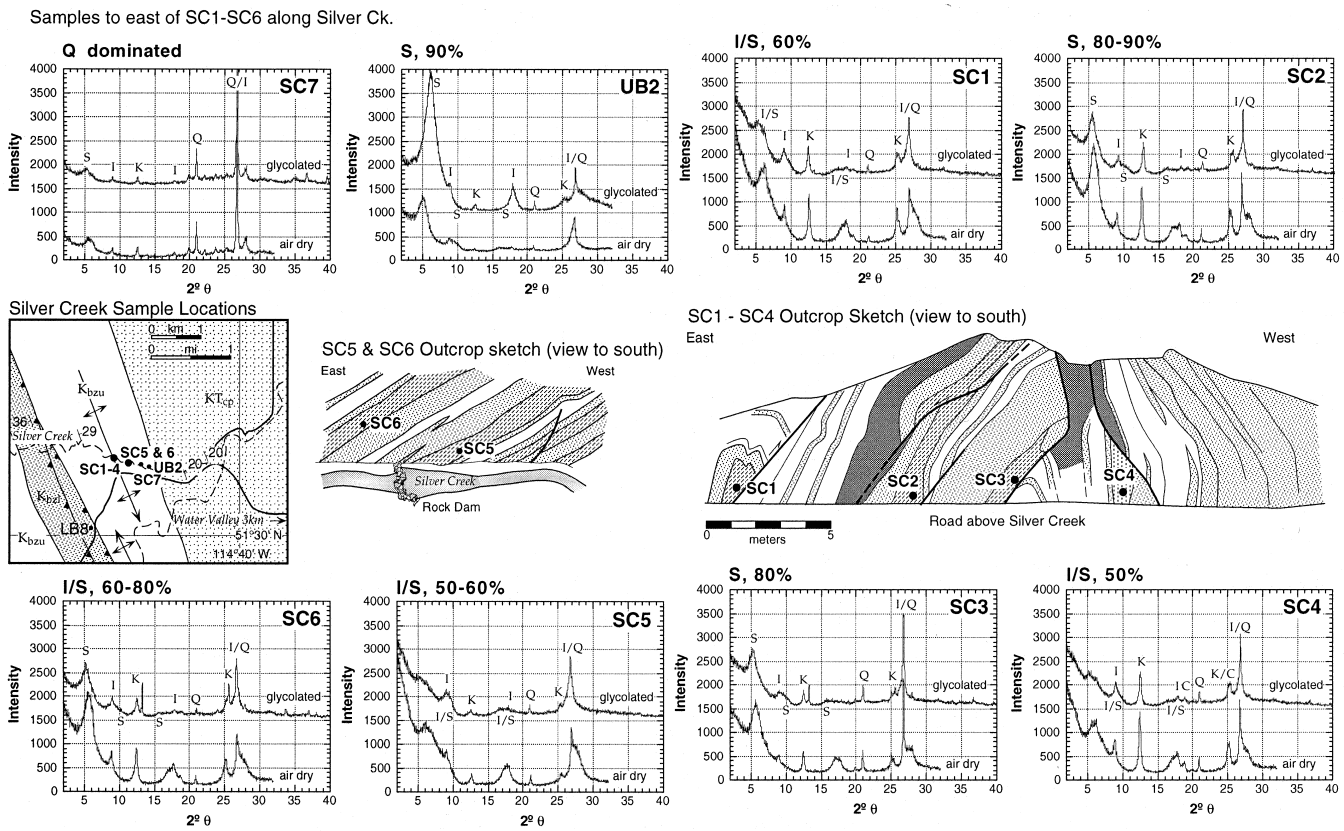

Fig. 6. Sketch of outcrop at the Silver Creek site showing the location of mudstone samples. Map shows the location of the outcrop and the location of other samples nearby (see Fig. 3 for map location). Graphs show the X-ray diffraction profiles for the clay fraction of each of the samples. Both the air dried and the glycolated profiles are shown for comparison. Symbols and labels as in Fig. 4. Interpretation of the percentage of smectite interlayers is shown at the top-left of each plot.

clays with 40–60% illite interlayers (Table 1). There is one exception to this. Sample BR38, from the Belly River Formation, which is the lower Brazeau Formation equivalent in the southern portion of the study area, contains almost 100% smectite (Table 1).

4.4. Alberta Group mudstones

Mudstones of the Alberta Group are also all located within thrust sheets of the Foothills belt (Fig. 11). These samples contain mixed-layer illite–smectite with at least 50% illite interlayers and in some cases almost pure illite (Fig. 13). Six of the 10 samples have diffraction profiles interpreted as having 70–80% or more illite interlayers in smectite.

4.5. Velocity and density profiles through the roof décollement

Three wells with sonic velocity logs and one with a density log penetrate through the roof décollement zone (Fig. 14a). The logs are hung on the K/T boundary. The location of the roof décollement zone was picked on seismic lines as the group of reflectors lying above those clearly in horse blocks and below those that are bent up with the cover (Figs. 2 and 14a). Near the top of the roof décollement, as picked on the seismic lines, there is a marked decrease in sonic velocity in all three of the wells. This corresponds to a decrease in density of about 75–100 kg/m^3 in well 16-14 (Fig. 14a). Beneath this drop in velocity and density, the velocity generally begins to rise again and it appears to level off above the BLRV marker (top lower Brazeau Formation, Fig. 2), near the base of the roof décollement. Since these rocks are in stratigraphic order, this break is not due to thrust superposition of deeper, more dense rocks.

5. Discussion

There is a clear break between strata that do and do not contain smectite-rich mudstones in the upper Brazeau Formation. With the exception of those near Tertiary synclines, all the upper Brazeau samples within thrust sheets contained mixed-layer clays. Therefore, it is reasonable to assume that this break is somewhere above the horse blocks, i.e. in the roof

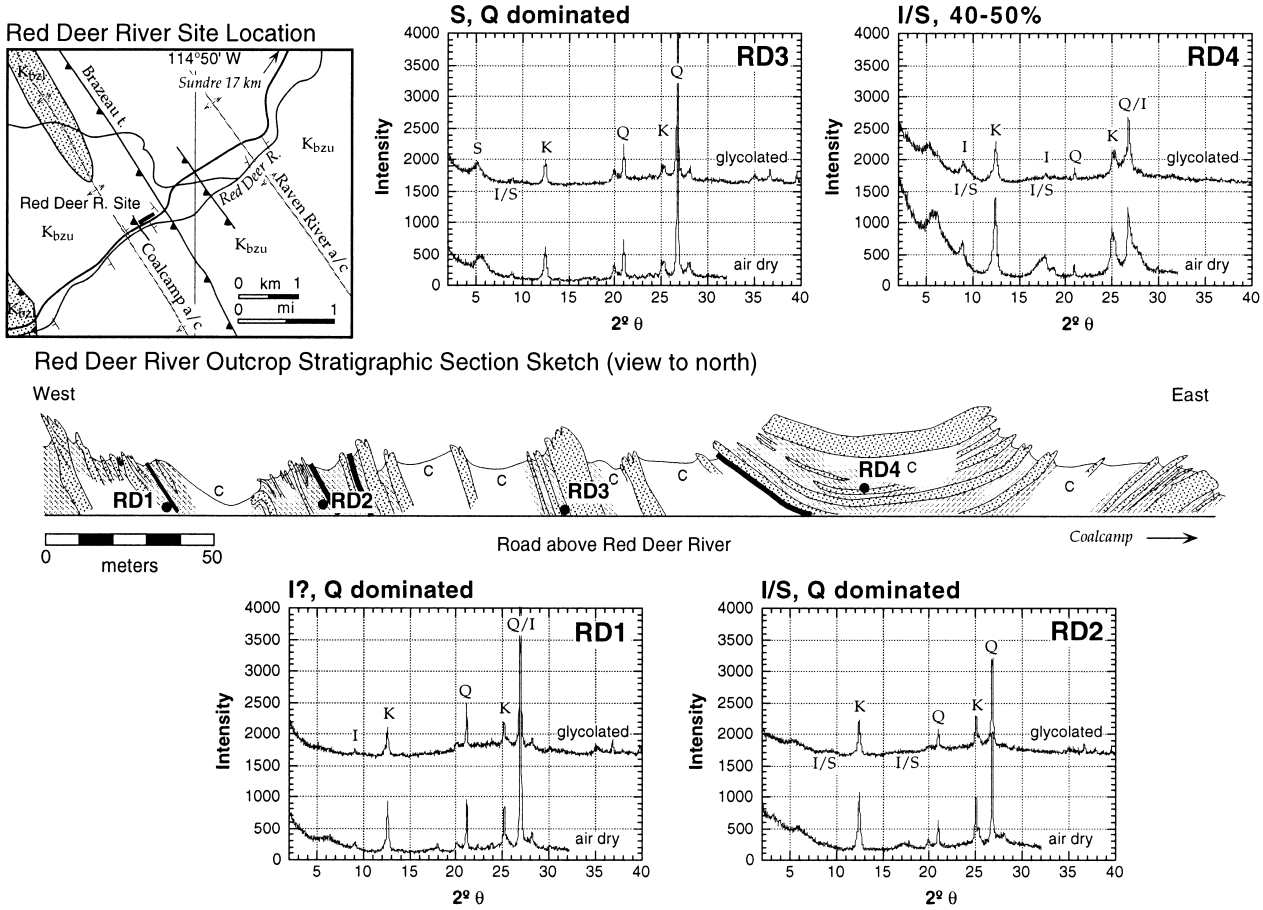

Fig. 7. Sketch of outcrop at the Red Deer River site showing the location of mudstone samples (see Fig. 3 for map location). Graphs show the X-ray diffraction profiles for the clay fraction of each of the samples. Both the air dried and the glycolated profiles are shown for comparison. Symbols and labels as in Fig. 4. Interpretation of the percentage of smectite interlayers is shown at the top-left of each plot.

décollement or cover (Fig. 11). This means that the horse blocks consist of stronger mudstones than those of the cover. Couzens and Wiltschko (1996) predicted that this relationship is a necessary condition for the formation of passive-roof duplexes.

Given that the type of clay changes in the stratigraphic section, the next question is whether the changes are due to deposition, diagenesis, or some combination of both. This is a concern because although smectite beds are not found beneath a certain stratigraphic level in the upper Brazeau Formation, they also are rare higher up in the Paskapoo Formation (Fig. 7). Similarly, where smectite-rich beds do occur, they are often interlayered with beds of mixed-layer clays (Figs. 5–7).

The correlation with sandstone petrology and the type of mudstone at a site argues strongly for a depositional control on the clay content within a mudstone. Where volcanic rock fragments and plagioclase clasts dominate the sandstones, smectite is present in the mudstones (Figs. 8 and 9). Where carbonate and sedimentary clasts dominate the sandstones, smectite is absent, and where both types of clasts are present, smectite is present in the mudstones to a lesser degree (Figs. 8 and 9). Without the source of abundant volcanic rocks and feldspar, smectite did not form and was not deposited. The increase in sedimentary rock fragments and loss of volcanic rock fragments is thought to be associated with renewed thrust motion in the Front Ranges and Foothills, which blocked off the distant volcanic rock source in the hinterland (Mack and Jerzykiewicz, 1989). In this case, mudstones from deeper levels, which are known to be smectite poor, would be uplifted, eroded and redeposited relatively locally as synorogenic deposits.

It is difficult, however, to attribute the loss of smectite within the upper Brazeau Formation to deposition alone. In particular, the amount of volcanic rock fragments and plagioclase clasts of the upper Brazeau sandstone beds does not decrease downward. Instead, it increases to a high of around 80% volcanic detritus just above the lower Brazeau Formation contact

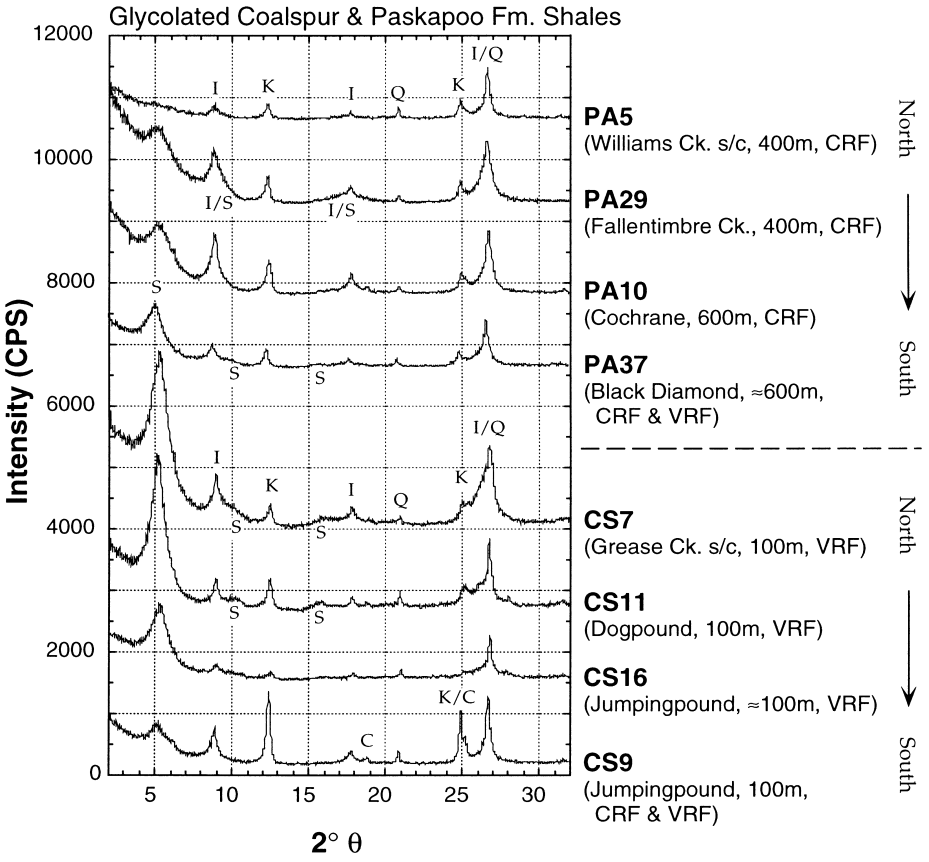

Fig. 8. X-ray diffraction profiles for the clay-size fraction of Paskapoo (PA) and Coalspur (CS) Formation samples. All profiles are of samples treated with ethylene glycol. Samples are shown by geographic locations, which can be found on the sample map (Fig. 3). The number next to the location indicates the approximate height above the Brazeau Formation contact. CRF — Carbonate rock fragments in nearby sandstones. VRF — Volcanic rock fragments in nearby sandstones. Labels on spectra as in Fig. 4.

(Mack and Jerzykiewicz, 1989), yet, smectite beds disappear altogether by this depth in the stratigraphy (Fig. 12).

The sequence of mineral changes during the S–I transition is unrelated to the depositional environment, stratigraphy or the age of the rocks (Velde, 1985). Younger rocks are not necessarily more smectitic; fully expandable clays can be found even in pre-Cambrian shales (van Moort, 1971; Velde, 1985). The main control on the transition is related to the highest physical conditions to which the rock has been exposed. In the case of the Alberta foreland basin, the rocks have been uplifted in thrust sheets, and the mountains have been denuded (Beaumont et al., 1985). However, we assume that the mudstones preserve the silicate mineral assemblage of their highest *P–T* conditions.

Coal moisture data and hydrocarbon isomerization and aromatization reactions provide constraints on the maximum *P–T* conditions that the rocks in the Foothills attained. In the Alberta foreland basin, coal moisture content studies indicate that 1.5–1.8 km of overburden has been removed near the Foothill thrust front (Hacquebard, 1977; Nurkowski, 1985). This places the Coalspur–Brazeau Formation contact at about 2 km maximum burial. Flexural models for the Alberta basin of Beaumont et al. (1985), which also use the coal moisture data to constrain the amount of erosion, are consistent with maximum burial depths predicted by aromatization and isomerization reactions in organic shales. Furthermore, the comparisons of flexural model predicted and observed ratios of product/(product + reactant) for the aromatization and isomerization reactions argues that the geothermal gradient in the basin has remained the same since Laramide time. The value computed by Beaumont et al. (1985) is about 27°C/km at the front of the Foothills.

To show that the mudstone units of the Alberta foreland basin have both undergone the S–I transition and preserved it we will compare observations in the Alberta foreland basin to those made in Gulf of Mexico sediments, where the S–I transition has been well documented. We chose the Gulf of Mexico for our comparison for a several of reasons. (1) The Gulf of Mexico is one of the best described and most studied S–I transitions. Not only is the transition well

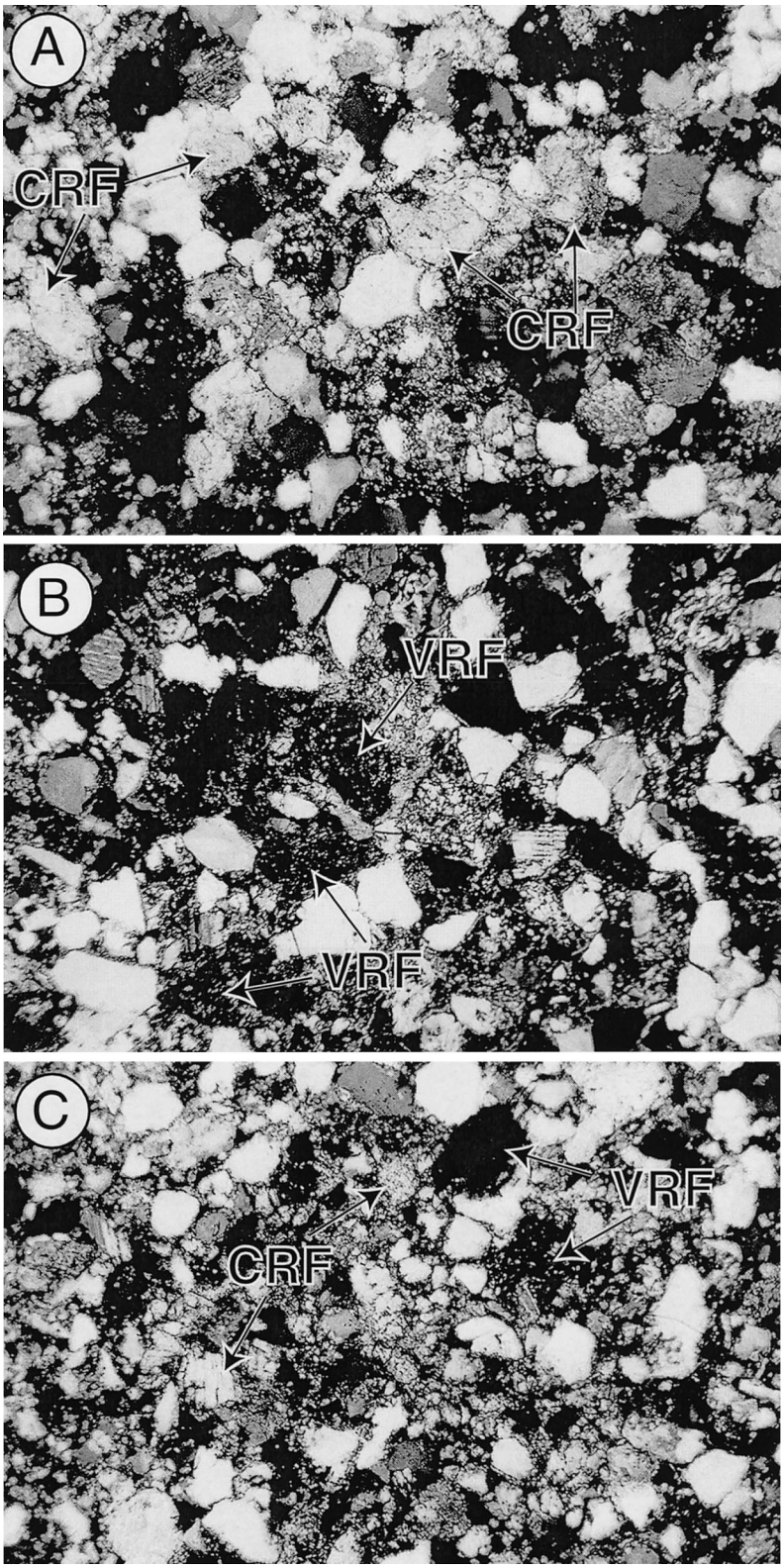

Fig. 9. Photomicrographs of sandstone samples located near shale samples. (a) Sandstone sample from the Paskapoo Formation with carbonate rock fragments. (b) Sandstone sample from the Coalspur Formation with volcanic rock fragments. (c) Sandstone sample from the Paskapoo Formation, south of the Bow River, with both volcanic and carbonate rock fragments. CRF — carbonate rock fragment. VRF — volcanic rock fragment.

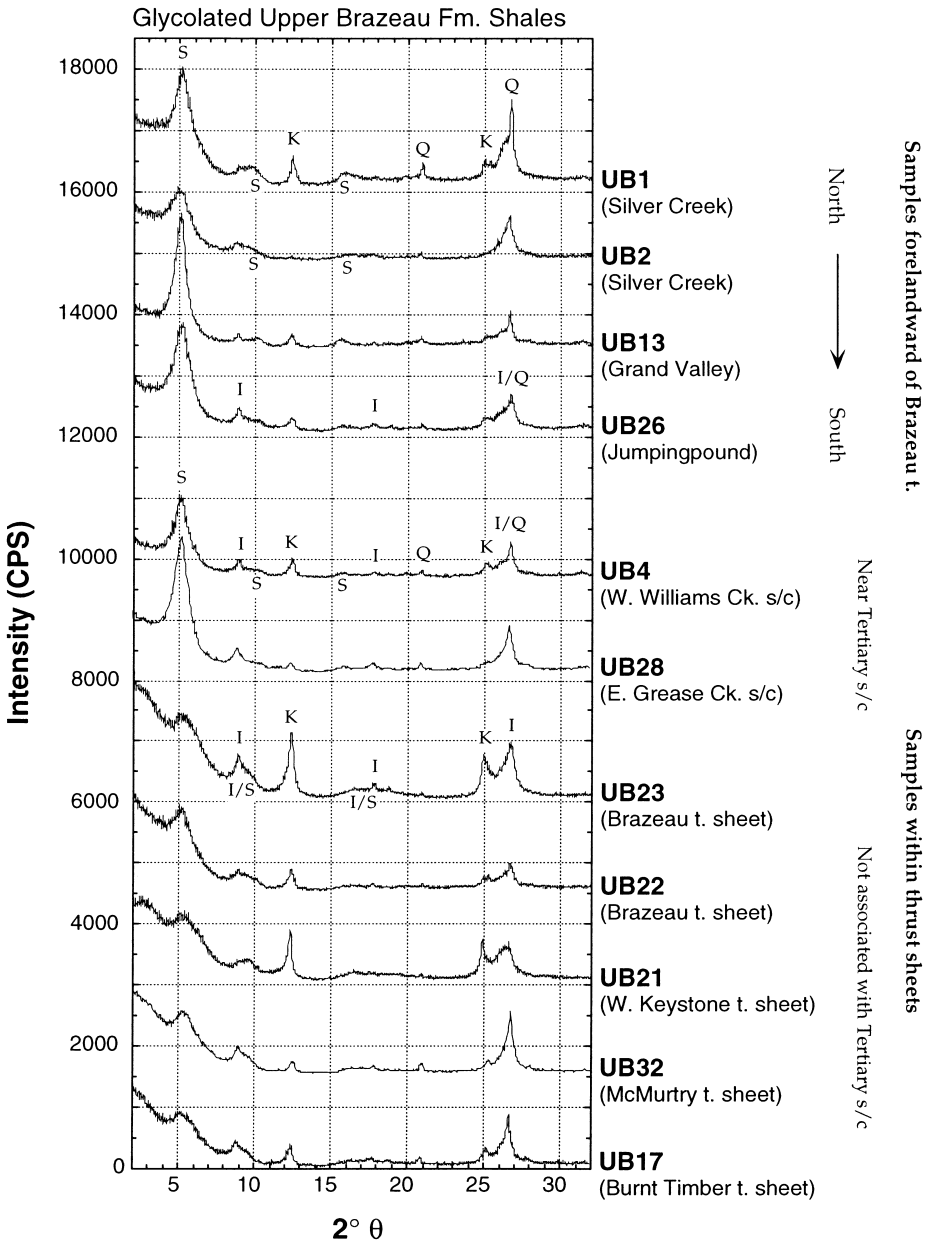

Fig. 10. X-ray diffraction profiles for the clay-size fraction of the upper Brazeau Formation (UB) samples. All profiles are of samples treated with ethylene glycol. Samples are shown by position within the Foothills thrust belt (see Fig. 11). Samples located forelandward of the most frontal thrust (Brazeau t.) and near synclines that preserve the Tertiary within the thrust belt are either in or above the roof décollement. Labels on spectra as in Fig. 4.

described there but its relationships to structural geometry and overpressures are also well documented. (2) The sedimentation type and rates are similar to those of the Cretaceous Foothills foreland. (3) Recently, several kinetic models have been developed to describe the S–I transition (e.g. Pytte, 1982; Velde and Vasseur, 1992; Huang et al., 1993). These models all have a similar form. They assume that loss of smectite equals a gain in illite on a molar basis (a non Al-conserved reaction). They all use an Arrhenius-type kinetic expression where the amount of smectite lost is dependent on the ratio of K^+/Na^+, temperature and time (Elliott and Matisoff, 1996). The models differ with respect to the overall order of the kinetic expression and to the term describing dependency of K^+ concentration for the transformation. Elliott and Matisoff (1996) evaluated the kinetic models and determined that: (i) none of the models works in all cases, i.e. site specific variables are sometimes necessary; and (ii) temperature is the dominate control on the reaction progress, whereas time is much less important. Because temperature is proportional to depth, the standard

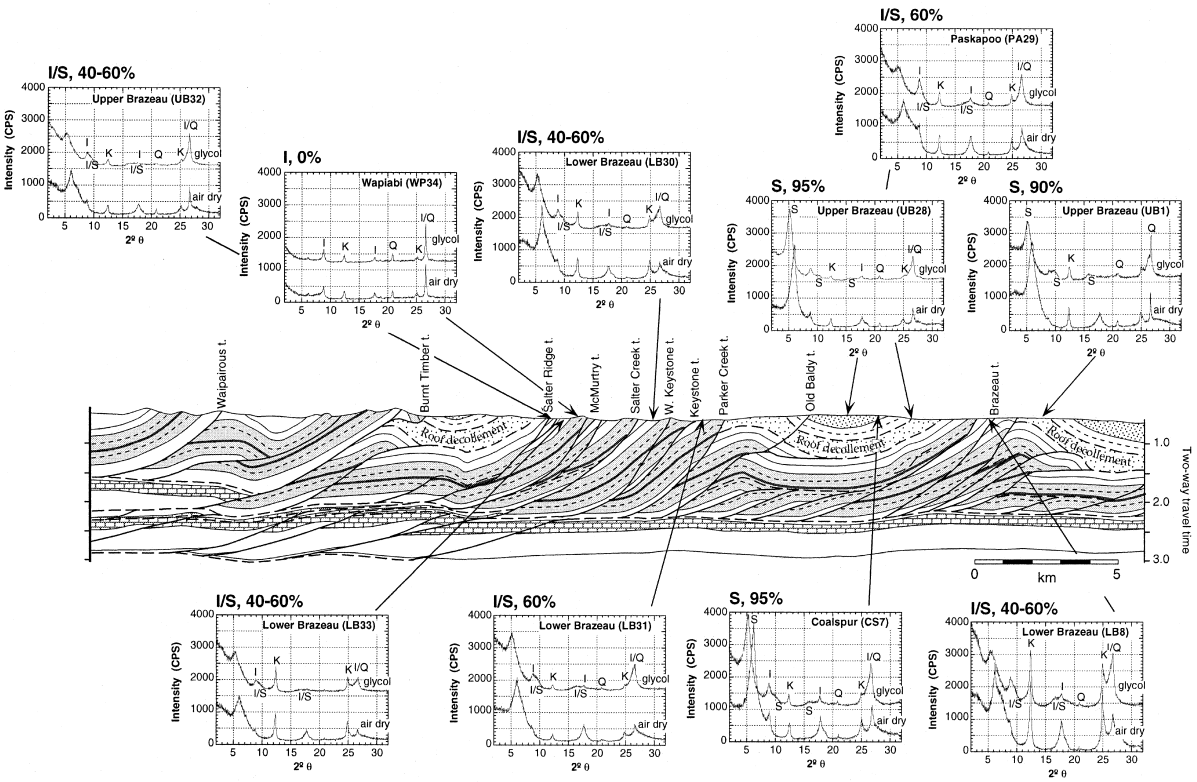

Fig. 11. Regional cross-section through the central Foothills thrust belt. The section is based on interpretation from seismic data, and has not been depth converted. The average velocity of the section is about 4000 m/s, yielding 1 km for 0.5 s two-way travel time; it has little to no vertical exaggeration. The section shows the relative positions of the main thrust sheets in the Foothills, the locations of nearby mudstone samples and their relation to the roof décollement. Graphs show the X-ray diffraction profiles for the clay fraction of each sample. Both air dried and the glycolated profiles are shown for comparison. Symbols and labels on spectra as in Fig. 4. On the cross-section, the bricks are the Mississippian, the dark gray shading is the Alberta Group and the thick black line is the Cardium Formation. The light gray shading is the roof décollement. The stipple is the Tertiary. Interpretation of the percentage of smectite interlayers is shown at the top-left of each plot.

depth oriented model for the S–I transition described by the transition in the Gulf of Mexico provides us with a reasonable point of comparison for the Alberta foreland.

In the Gulf of Mexico, there are several common attributes of the S–I transition and its relation to other physical properties:

1. There is a change from >80% expandable clays to <20% expandable clays over a 1400 m interval (Fig. 14b; Hower et al., 1976; Bruce, 1984).
2. In a general way, X-ray diffraction patterns show that unordered interlayered clays are succeeded by ordered ones with increasing depth as follows (Fig. 14c; Velde, 1985): (i) smectite or mixed-layer clays with less than 30% random interlayers of illite; (ii) ordered expandable interlayers between 40 and 60% smectite in composition; (iii) allevardite- or IS-type minerals with 20–40% expandable interlayers; (iv) ISII-type minerals with less than 10% smectite. Based on TEM observations across the transition, Ahn and Peacor (1986) propose that the transition is gradual as illite grows at the expense of smectite. Although the transition is gradual, the distinct XRD patterns of the four stages above correspond to a series of changes in the initially heterogeneous assemblage of smectite. The succession starts with 'megacrystals' of anastomosing interlayers of smectite and random illite/smectite that form a continuous matrix with abundant defects. With burial or tectonic stress, the smectite layers are replaced with relatively defect free illite domains that grow by diffusion of K^+ and Al^{3+} through the smectite megacrystal (Ahn and Peacor, 1986). At about 50% illite-like layers, packets of illite form thin lath-like pseudohexagonal euhedral to subhedral plates. This is the first detectable order (Peacor, 1992) and gives rise to the second XRD pattern. As the packets begin to increase in size, they interlock and form illite-like layers that are a few tens of nanometers thick (Peacor, 1992), causing the third XRD pattern. Finally, recrystallization of illite or ordered illite/smectite forms larger interlocking crystals of white mica (Peacor, 1992).
3. The S–I transition begins to occur at temperatures between 65°C and 90°C. At this point mixed-layer clays with 40–60% expandable interlayers appear.

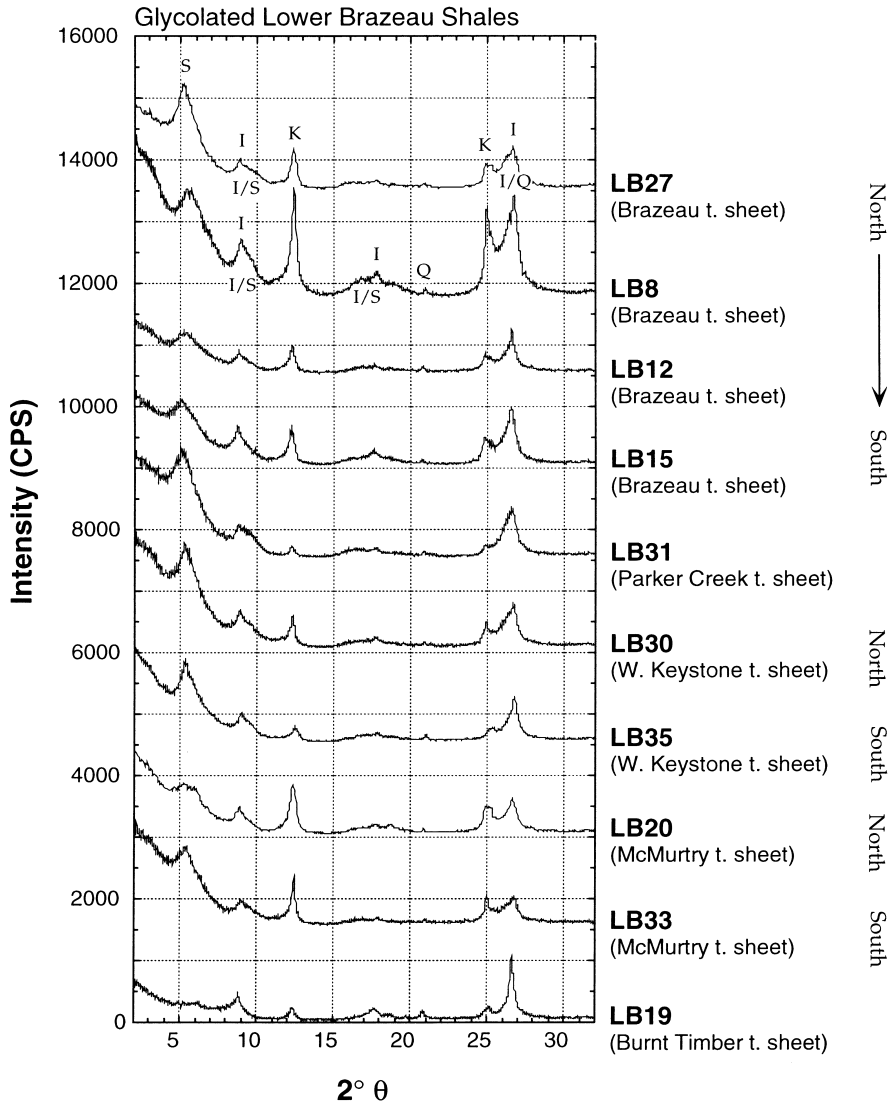

Fig. 12. X-ray diffraction profiles for the clay-size fraction of the lower Brazeau Formation (LB) samples. All profiles are of samples treated with ethylene glycol. Samples are shown by position within the Foothills thrust belt (see Fig. 11). Labels on spectra as in Fig. 4.

The S–I transition is much more sensitive to changes in temperature than to changes in pressure (Fig. 14c; e.g. Bruce, 1984).

4. There is a corresponding rapid drop in shale density at the transition (Schmidt, 1973), which generally increases with depth and compaction. Similarly, there is an associated increase in porosity (Fig. 14b; Schmidt, 1973; Bruce, 1984).
5. The S–I transition corresponds to the top of an overpressured zone in several Gulf of Mexico examples including: (i) a Miocene silty sandstone–shale section (Bruce, 1984); (ii) the Oligocene section of south Texas (Berg and Habeck, 1982); and (iii) in a well in Brazoria county, Texas (Freed, 1982). The correlation is not recognized where there are sufficient permeable sandstone beds to act as conduits for fluid egress (Bruce, 1984). Where overpressure does develop, the coalescing illite mats within the smectite megacrystals are thought to create a seal that traps both water produced by transformation and formation water trying to escape from the compacting sediments below (Freed and Peacor, 1989a).
6. Normal faults change orientation and flatten from 50–60° dips to 10–15° dips through the S–I transition and associated overpressured shale. In some cases the faults may even become bed-parallel (Bruce, 1984).

In the mudstones of the Alberta foreland basin, there is a definite succession of X-ray diffraction patterns over about 1000–1500 m of section. Beds at the top contain both smectite-rich horizons and smectite-poor horizons in the Paskapoo, Coalspur and upper Brazeau Formations (Figs. 8 and 10). In the middle, beds contain mixed-layer clays with 40–60% expand-

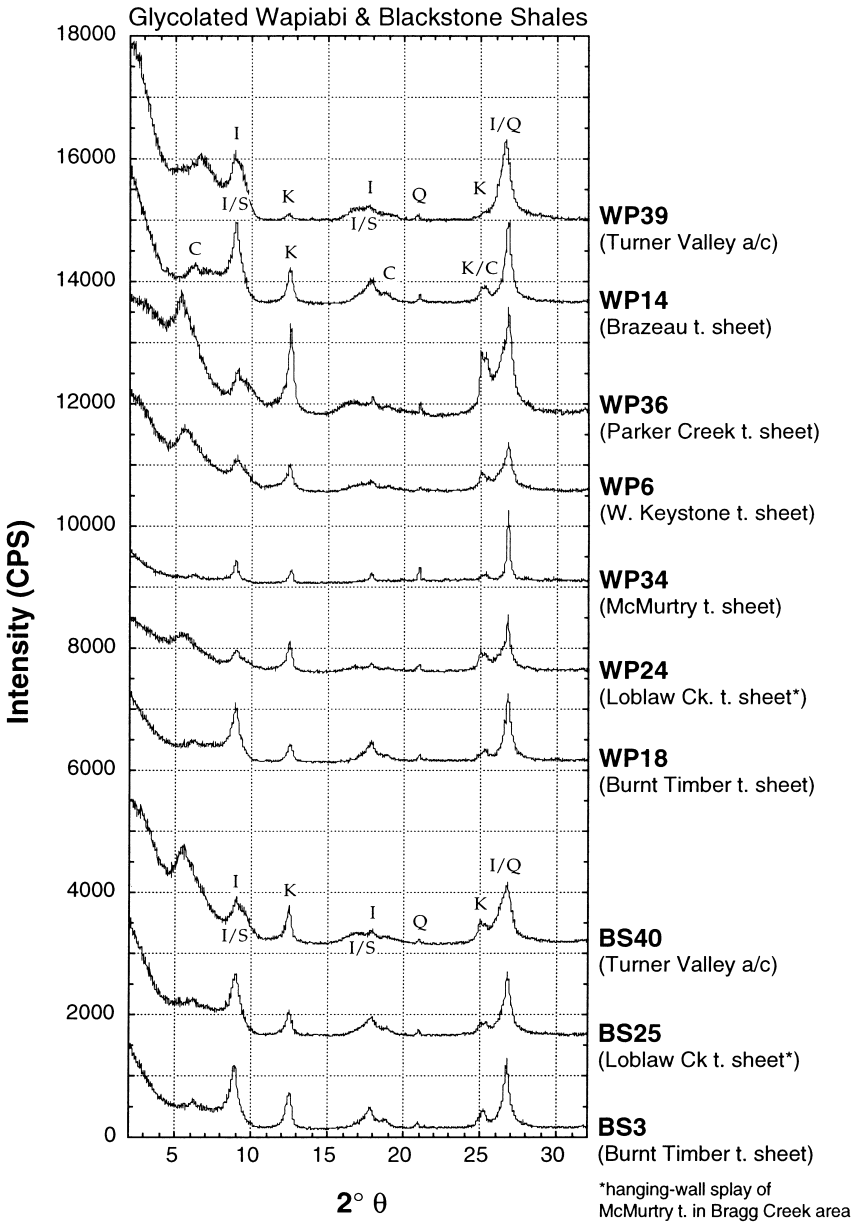

Fig. 13. X-ray diffraction profiles for the clay-size fraction of the Alberta Group (WP & BS) samples. All profiles are of samples treated with ethylene glycol. Samples are shown by position within the Foothills thrust belt (see Fig. 11). Labels on spectra as in Fig. 4.

able interlayers in the upper and lower Brazeau Formation (Figs. 10 and 12). Finally, in the Alberta Group, beds contain ordered IS-type minerals with 20–30% smectite interlayers (Fig. 13, Table 1). This succession with depth of different X-ray diffraction patterns for smectitic clays matches that of several previous studies, with the exception that the clay content of the upper beds in this study is controlled by source rock type.

Based on data from previous studies (see Velde, 1985), the locations of these transitions of X-ray diffraction patterns are shown in temperature–depth space on Fig. 14(c). Note that Fig. 14(c) is not a true phase diagram. Equilibrium has not been demonstrated for smectite–I/S–illite reactions (Essene and Peacor, 1995). However, the diagram is still useful as a general index of maximum temperature (Essene and Peacor, 1995). Given the maximum burial of the Coalspur–Brazeau Formation contact at about 2 km, and a geothermal gradient of about 30°C/km, we can predict the locations of the transformations in the stratigraphic section on Fig. 14(c). The transition from smectite to mixed-layer clays should occur in the top portion of the upper Brazeau, in agreement with observation (Figs. 10 and 11). Likewise, the transition to IS-type clays, with 20–40% smectite, should occur near

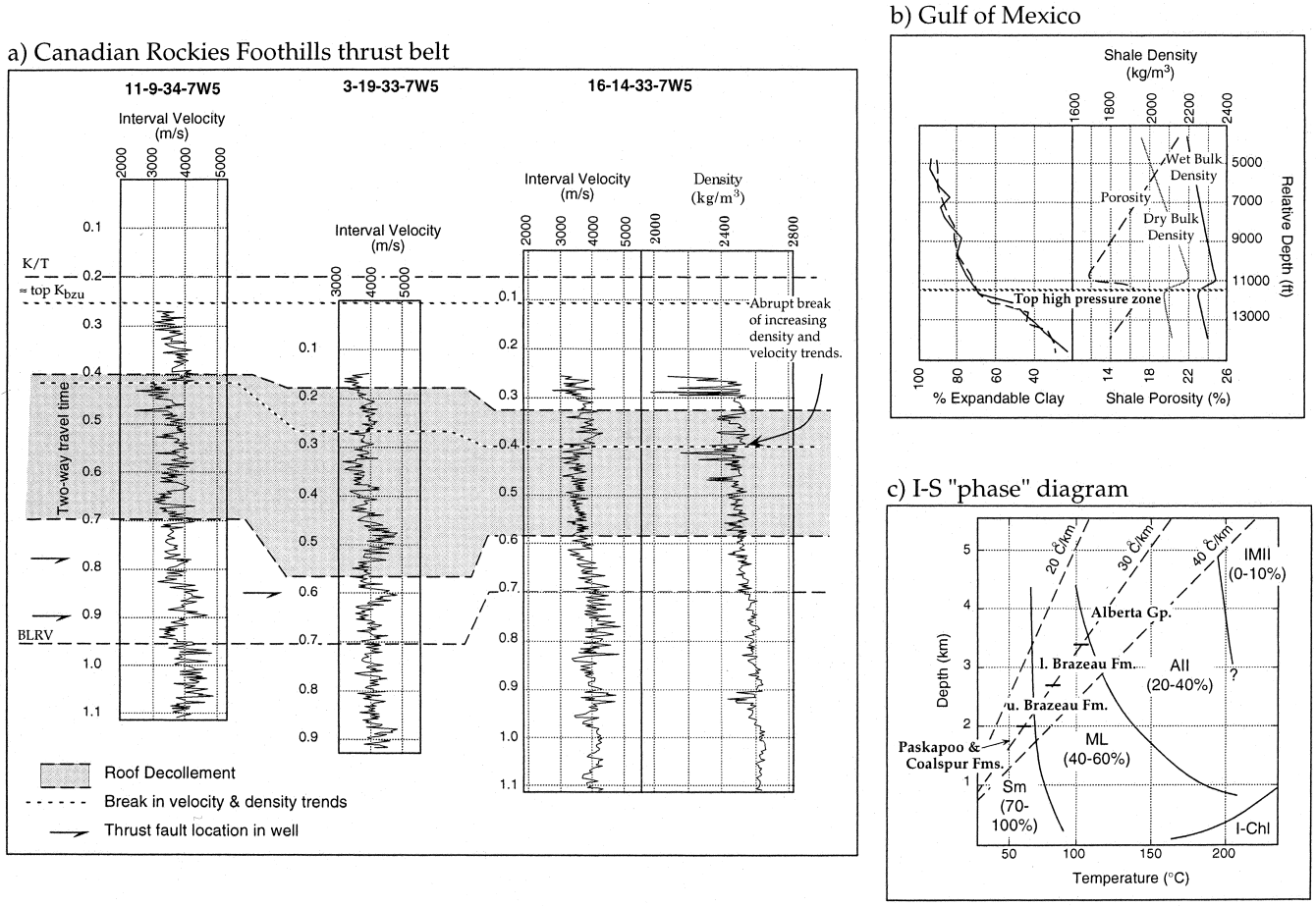

Fig. 14. Correlation of the S–I transition and density. (a) Velocity logs and density log from wells that penetrate the cover unit, through the roof décollement and into the horse blocks beneath. Location of the wells is shown on Fig. 2. The logs are hung on the K/T boundary, with the shaded region showing the location of rocks within the roof décollement (as picked on Fig. 2). Kbzu — top upper Brazeau Formation. BLRV — approximate top lower Brazeau Formation (= top Belly River Formation). Arrows show where thrust faults repeat the section. (b) Plot of shale density and porosity as it relates to the S–I transition in the Gulf of Mexico sediments (Schmidt, 1973). (c) Diagram showing the fields for smectite, illite and mixed-layer clays based on X-ray diffraction patterns from clay samples from both deep drill holes and drill holes in hydrothermal areas. Sm — smectite, ML — ordered mixed-layer, All — allevardite type clays (IS), IMII — less that 10% smectite (ISII), I-Chl — illite–chlorite facies (Velde, 1985, from work of Dunoyer de Segonzac, 1969; Iijima, 1970; Perry and Hower, 1970, 1972; van Moort, 1971; Weaver and Beck, 1971; Schmidt, 1973; Hower et al., 1976; Yeh and Savin, 1977; Boles and Franks, 1979; Aoyagi and Kazama, 1980; Lahann, 1980).

the top of the Alberta Group, also in agreement with our observations (Figs. 13 and 11).

At the southern edge of the study area (Turner Valley) smectite was found slightly deeper in the section, namely, in the Belly River Formation (Table 1). This fact suggests that the S–I transition is slightly deeper there. Samples from the Alberta Group in the same area have mixed-layer clays with about 20–40% expandable interlayers, similar to other Alberta Group samples. The appearance of Allevardite-type clays in the Alberta Group at Turner Valley seems to imply that the transition occurred over a thinner sequence of rocks. However, the stratigraphic section also thickens to the south (Mack and Jerzykiewicz, 1989).

The apparent drop of the S–I transition to a lower stratigraphic level could result from a lower geothermal gradient to the south (Fig. 14b). This would not, however, easily explain any thinning of the transition. Aside from temperature, other properties, such as changes in fluid compositions, porosity, or permeability affect the kinetics that control the flow of ions within smectite domains and between illite and smectite domains (Ahn and Peacor, 1986). As a result, changes in those properties also have the potential to affect the location of I–S transition.

Whatever the cause of the apparent stratigraphic drop in the location of the S–I transition, the drop also correlates with a drop in the location of the roof décollement in the Foothills (MacKay et al., 1994). The décollement also changes seismic character to the

south. Instead of being a thick zone of deformed beds, its thickness is below the resolution of seismic reflection data. This may reflect the thinning of the S–I transition zone. On the other hand, the décollement may be more localized because the rocks in the area are stronger in general. The sandstones in the south have fewer volcanic sourced clasts so most of the mudstones are probably less smectite-rich causing the whole section to be stronger.

Other related changes in properties across the proposed transition improve the correlation between the S–I transition and the formation of the roof décollement. In the Gulf of Mexico, the density of the shale abruptly drops just above the start of the transition and then begins to increase again continuing down section (Fig. 14b). Similarly, porosity abruptly increases at the start of the transition and then begins to decrease (Schmidt, 1973). We would predict this to occur in the Foothills within the upper Brazeau Formation, somewhere within the roof décollement. We have three wells with sonic velocity data and one with density data that penetrate the roof décollement in the north end of the study area (Fig. 14a). There is an abrupt break in the density trend in the latter well. The density decreases at this break by about 75 kg/m^3, similar to the drop in density seen in the Gulf of Mexico at the start of the S–I transition. There is also an abrupt decrease in sonic velocity trend at the location of the break in the density trend (Fig. 14a).

Breaks in the sonic velocity trend are seen in the other two wells that penetrate the roof décollement. The top of the roof décollement was picked on reflection seismic lines as the base of the last reflector associated with the gently east-dipping cover rocks. Relative to this reflector, the break in trend in the three examples occurs about 100–200 m (0.05–0.1 s two-way travel time) beneath the top of the roof décollement (Fig. 14a). A similar disruption in velocity trends also appears to be present in well logs through the roof décollement zone near the Bow River (Lawton et al., 1994). Again, a break is found within the upper Brazeau Formation underneath the last clear reflectors in the cover (Lawton et al., 1994).

The breaks in trend are small, compared to the variation in density and velocity. However, we believe there is a shift in the entire trend, which also shifts the maxima and minima by 75–100 kg/m^3. Because the drop is similar to that in the Gulf of Mexico, we propose that, as in the Gulf of Mexico, it is preserving undercompaction of the mudstones related to the S–I transition. The shifts in trend, however, are simply another piece of permissive evidence. Other breaks in the velocity trends exist (e.g. well 3-19-33-7W5, Fig. 14), and other lithology changes could have similar effects. None-the-less, in our three example wells and in both the wells near the Bow River the break in trend is consistently just beneath the last continuous reflector in the cover rocks.

The drop in density and velocity trends across the roof décollement could be reflecting either: (i) dilation in the roof décollement due to deformation; or (ii) undercompaction due to overpressuring of the shale at the top of the I–S transition. By analogy with the Gulf of Mexico, we favor the latter. In the Gulf of Mexico sediments, we noted that both the break in density and porosity trends and the appearance of mixed-layer clays (40–60% expandable interlayers) correlate with the top of overpressured shales (Berg and Habeck, 1982; Freed, 1982; Bruce 1984). This occurs where shales are continuous enough that the sandstones present do not provide a coherent exit path for fluids. Given that the Brazeau Formation contains 40–50% shale and coal with channel sands, it is possible that the section could have become overpressured. The result would be to create a zone favorable for detachment in a section of otherwise monotonous rocks. Similar to the Gulf of Mexico, the deformation styles of the rocks above and below the transition are different. The section beneath the S–I transition is thrust faulted, the thrust faults merging with the roof décollement at the S–I transition. The rocks above are folded over the thrust faulted structures beneath.

6. Conclusions

1. A correlation exists between the S–I transition and the location of the roof décollement in the Foothills of the Canadian Rockies. (a) Outcrops above the roof décollement contain both smectite-rich shales and smectite-poor shales. The variability is attributed to sedimentary provenance differences. Smectite-rich shales are associated with sandstones that have volcanic source rocks in the hinterland. Smectite-poor shales are associated with sandstones that have local sedimentary source rocks in the foreland thrust belt. The loss of smectite in the Paskapoo Formation north of the Bow River correlates with a loss of volcanic rock fragments in the associated sandstones, which is thought to reflect renewed thrust motion that cut off the hinterland source of volcanics (c.f. Mack and Jerzykiewicz, 1989). (b) Outcrops beneath the roof décollement in the Brazeau Formation contain mixed-layer clays with 40–60% expandable smectite interlayers. However, the associated sandstones still contain abundant volcanic rock fragments, similar to those sandstones above the roof décollement that are associated with smectite-rich shale. We believe that the shales beneath the roof décollement were originally smecti-

tic, but have begun the transition from smectite to illite. (c) Stratigraphically deeper outcrops in the Alberta Group shales have only 20–30% smectite interlayers. We propose that these shales have almost completely gone through the S–I transition. Our correlation is similar to previous correlations in accretionary prisms between the location of the basal décollement and the base of smectite-rich sediments (e.g. Tribble, 1990; Vrolijk, 1990; Wilkens et al., 1990). The correlation is permissable evidence that the S–I transition controlled the formation and location of the roof décollement to passive-roof duplexes in the Foothills. The possibility that some other mineralogical change is causing localization of the décollement still exists. This could be examined by looking at the silt fractions in a whole rock analysis study. However, since we see little change in the sandstone petrology of the Brazeau Formation (c.f. Mack and Jerzykiewicz, 1989), we believe it is reasonable to assume that the silts do not drastically change either.

2. The succession from smectite-rich to mixed-layer clays with 40–60% expandable interlayers to allevardite-type clays with 20–30% expandable interlayers matches the observations of several previous studies of the S–I transition. The change from $>80\%$ expandable clays to $<20\%$ expandable clays takes place over a similar thickness. The locations of the changes in the Foothills stratigraphy are consistent with the predicted locations based on inferred maximum burial conditions from coal moisture content and hydrocarbon aromatization and isomerization reactions in organic shales (c.f. Hacquebard, 1977; Nurkowski, 1985; Beaumont et al., 1985).
3. A break in the density trend, and a corresponding break in the sonic velocity trend correlates to the top of the S–I transition in the Foothills. This break in the density trend has also been documented at the top of the S–I transition in the Gulf of Mexico, where it also corresponds to a zone of overpressure. The break in the foothills trend is of a similar magnitude to that documented in the Gulf of Mexico. Overpressuring makes the transition a favorable zone for detachment in the Gulf of Mexico. There, normal faults change orientation, becoming more bed-parallel across the transition. Similarly, in the Foothills, thrust faults flatten into the top of the transition zone and disperse their shortening into smaller structures. We propose that the drop in density seen at the top of the transition in the Foothills records a paleo-overpressured horizon that made it favorable for detachment and formation of the roof décollement to the Foothills triangle zone.

Acknowledgements

We thank T. Radford and Amoco Canada Ltd. For providing seismic data and well logs, John Panian for field assistance, and both Caesar Williams and Judith Smith for laboratory assistance. D.V.W. thanks D. Peacor for many stimulating discussions on clay diagenesis during a sabatical stay at The University of Michigan. We thank Dennis Johnston and Peter Vrolijk for reviews that improved the final version of the manuscript. This work was partially supported by NSF grant 94-05162 to Wiltschko and by grants from Amoco Petroleum Co. and Atlantic Richfield Co. to Couzens-Schultz.

References

Ahn, J.H., Peacor, D.R., 1986. Transmission and electron microscopy of the smectite-to-illite transition. Clays and Clay Minerals 34, 165–179.

Aoyagi, K., Kazama, T., 1980. Transformational changes of clay minerals. Zeolites and silica minerals during diagenesis. Sedimentology 27, 179–188.

Bally, A.W., Gordy, P.L., Stewart, G.A., 1966. Structure, seismic data and orogenic evolution of the southern Canadian Rocky Mountains. Bulletin of Canadian Petroleum Geology 14, 337–381.

Beaumont, C., Boutilier, R., MacKanzie, A.S., Rullkötter, J., 1985. Isomerization and aromatization of hydrocarbons and the paleothermometry and burial history of the Alberta foreland basin. American Association of Petroleum Geologists Bulletin 69, 546–566.

Berg, R.R., Habeck, M.F., 1982. Abnormal pressures in the lower Vicksburg, McAllen Ranch field, south Texas. Gulf Coast Association of Geological Societies Transactions 32, 247–253.

Boles, J.R., Franks, S.G., 1979. Clay diagenesis in Wilcox sandstones of southwest Texas: Implications of smectite diagenesis on sandstone cementation. Journal of Sedimentary Petrology 49, 55–70.

Bruce, C.H., 1984. Smectite dehydration — its relation to structural development and hydrocarbon accumulation in Northern Gulf of Mexico basin. American Association of Petroleum Geologists Bulletin 68, 673–683.

Burst, J.F., 1969. Diagenesis of Gulf Coast clayey sediments and its possible relation to petroleum migration. American Association of Petroleum Geologists Bulletin 53, 73–93.

Carrigy, M.A., 1971. Lithostratigraphy of the uppermost Cretaceous (Lance) and Paleogene strata of the Alberta Plains. Research Council of Alberta Bulletin 27.

Couzens, B.A., Wiltschko, D.V., 1996. The control of mechanical stratigraphy on the formation of triangle zones. Bulletin of Canadian Petroleum Geology 44, 165–179.

Clarke, G.B., 1966. Deformation moduli of rocks. In: Testing Techniques for Rock Mechanics—ASTM 5th Pacific Area National Meeting, Seattle, American Society for Testing and Materials Special Technical Publication 402, Philadelphia, Pennsylvania, pp. 133–172.

Dechesne, R.G., Muraro, J.W., 1996. A relict triangle zone at Benjamin Creek gas field, southern Alberta Foothills: Geometry, kinematics and preservation. Bulletin of Canadian Petroleum Geology 44, 269–281.

Dunoyer de Segonzac, G., 1969. Les minéraux argileux dans la diagénèse; passage au métamorphisme. Thesis, University of

Strasbourg. Mémoirs du Service Carte Géologique d'Alsace–Lorraine 29, Strasbourg, France.

Elliott, W.C., Matisoff, G., 1996. Evaluation of kinetic models for the smectite to illite transformation. Clays and Clay Mineralogy 44, 77–87.

Essene, E.J., Peacor, D.R., 1995. Clay mineral thermometry—A critical perspective. Clays and Clay Minerals 43, 540–553.

Evamy, B.D., Haremboure, J.P., Kamerling, W.A., Knaap, F.A., Molloy, F.A., Rowlands, P.H., 1978. Hydrocarbon habitat of Tertiary Niger delta. American Association of Petroleum Geologists Bulletin 62, 1–39.

Freed, R.L., 1982. Clay mineralogy and depositional history of the Frio formation in two geopressured wells Brazoria County, Texas. Gulf Coast Association of Geological Societies Transactions 32, 459–463.

Freed, R.L., Peacor, D.R., 1989a. Geopressured shale and sealing effect of smectite to illite transition. American Association of Petroleum Geologists Bulletin 73, 1223–1232.

Freed, R.L., Peacor, D.R., 1989b. Variability in temperature of the smectite/illite reaction in Gulf Coast sediments. Clay Minerals 24, 171–180.

Hacquebard, P.A., 1977. Rank of coal as an index of organic metamorphism for oil and gas in Alberta. In: Deroo, G., Powell, T.G., Tissot, B., McCrossan, R.G. (Eds.), The Origin and Migration of Petroleum in the Western Canada Sedimentary Basin, Bulletin of the Geological Survey of Canada 262, pp. 11–22.

Hower, J., 1981. X-ray diffraction identification of mixed-layer clay minerals. In: Longstaffe, F.J. (Ed.), Short Course in Clays and the Resource Geologist. Mineralogical Association of Canada, Calgary, Alberta, pp. 39–80.

Hower, J., Eslinger, E.V., Hower, M.E., Perry, E.A., 1976. Mechanism of burial metamorphism of argillaceous sediment 1: Mineralogical and chemical evidence. Geological Society of America Bulletin 87, 725–737.

Huang, W.-L., Longo, J.M., Pevaer, D.R., 1993. An experimentally derived kinetic model for the smectite-to-illite conversion and its use as a geothermometer. Clays and Clay Minerals 41, 162–177.

Iijima, A., 1970. Present day zeolitic diagenesis of the Neogene geosynclinal deposits in the Niigata oil field, Japan. American Chemical Society 2nd International Zeolite Conference, 540–546.

Inoue, A., Bouchet, A., Velde, B., Meunier, A., 1989. Convenient technique for estimating smectite layer percentage in randomly interstratified illite/smectite minerals. Clays and Clay Minerals 37, 227–234.

Jackson, M.L., 1969. Soil Chemical Analysis—Advanced Course. Published by the author, Department of Soils, University of Wisconsin, Madison.

Jerzykiewicz, T., 1985. Stratigraphy of the Saunders Group in the central Alberta Foothills—a progress report. In: Current Research Part B. Geological Survey of Canada Paper 85-1B, pp. 247–258.

Kerr, P.E., Barrington, J., 1961. Clays of deep shale zone, Caillou Island, Louisiana. . American Association of Petroleum Geologists Bulletin 45, 1697–1712.

Lahann, R.W., 1980. Smectite diagenesis and sandstone cement: The effect of reaction temperature. Journal of Sedimentary Petrology 50, 755–760.

Lawton, D.C., Spratt, D.A., Hopkins, J.C., 1994. Tectonic wedging beneath the Rocky Mountain foreland basin, Alberta, Canada. Geology 22, 519–522.

Mack, C., Jerzykiewicz, T., 1989. Provenance of post-Wapiabi sandstones and its implications for Campainian to Paleocene tectonic history of the southern Canadian Cordillera. Canadian Journal of Earth Sciences 26, 665–677.

MacKay, P.A., 1996. The Highwood structure: A tectonic wedge at the foreland edge of the southern Canadian Cordillera. Bulletin of Canadian Petroleum Geology 44, 215–232.

MacKay, P.A., Spratt, D.A., Soule, G.S., Lawton, D.C., 1994. The triangle zone of southern Alberta — geometry, lateral variations and associated oil and gas fields. Fieldtrip Guidebook Canadian Society of Economic Geologists/Canadian Society of Petroleum Geologists Convention, Calgary, Alberta.

McMechan, M.E., 1995. Geology, Rocky Mountain Foothills and Front Ranges in Kananaskis Country, Alberta. Geological Survey of Canada Map 1865A.

Nurkowski, J.R., 1985. Coal quality and rank variation within upper Cretaceous and Tertiary sediments, Alberta plains region. Alberta Research Council Earth Science Report 85-1.

Ollerenshaw, N.C., 1965. Geology, Burnt Timber Creek. Geological Survey of Canada Map 11-1965.

Ollerenshaw, N.C., 1969. Geology, Marble Mountain. Geological Survey of Canada Map 7-1969.

Ollerenshaw, N.C., 1972. Geology, Wildcat Hills (west half). Geological Survey of Canada Map 1351A.

Ollerenshaw, N.C., 1974. Geology, Fallentimber Creek (west half). Geological Survey of Canada Map 1387A.

Ollerenshaw, N.C., 1975. Rocky Mountain Foothills and Front Ranges compilation map. In: Evers, H.J., Thorpe, J.E. (Eds.), Structural Geology of the Foothills Between Savana Creek and Panther River S.W. Alberta Canada, Canadian Society of Petroleum Geologists and Canadian Society of Exploration Geophysicists Guidebook "Exploration Update 75".

Ollerenshaw, N.C., 1978. Geology, Calgary, Alberta–British Columbia. Geological Survey of Canada Map 1457A.

Peacor, D.R., 1992. Diagenesis and low-grade metamorphism of shales and slates. In: Buseck, P.R. (Ed.), Mineral Reactions at the Atomic Scale: Transmission Electron Microscopy, Reviews in Mineralogy 27. Mineralogical Society of America, Washington, DC, pp. 335–380.

Perry, E.A., Hower, J., 1970. Burial diagenesis in Gulf Coast pelitic sediments. Clays and Clay Minerals 18, 165–177.

Perry, E.A., Hower, J., 1972. Late stage dehydration in deeply buried pelitic sediments. American Association of Petroleum Geologists Bulletin 56, 2013–2021.

Pollastro, R.M., 1985. Mineralogical and morphological evidence for the formation of illite at the expense of illite/smectite. Clays and Clay Minerals 33, 265–274.

Powers, M.C., 1967. Fluid release mechanisms in compacting marine mudrocks and their importance in oil exploration. American Association of Petroleum Geologists Bulletin 51, 1240–1254.

Pytte, A., 1982. The kinetics of the smectite to illite reaction in contact metamorphic shales. Unpublished M.S. Thesis, Dartmouth College, Hanover, New Hampshire.

Schmidt, G.W., 1973. Interstitial water composition and geochemistry of deep Gulf Coast shales and sandstones. American Association of Petroleum Geologists Bulletin 57, 321–337.

Shaw, E.W., 1963. In: Childs, O.E. (Ed.), Canadian Rockies — orientation in time and space; Backbone of the Americas, American Association of Petroleum Geologists Memoir 2, pp. 231–242.

Shimamoto, T., Logan, J.M., 1981. Effects of simulated clay gouges on the sliding behavior of the Tennessee sandstone. Tectonophysics 75, 243–255.

Slotboom, R.T., Lawton, D.C., Spratt, D.A., 1996. Seismic interpretation of the triangle zone at Jumping Pound, Alberta. Bulletin of Canadian Petroleum Geology 44, 233–243.

Soule, G.S., Spratt, D.A., 1996. En échelon geometry and two-dimensional model of the triangle zone, Grease Creek syncline area, Alberta. Bulletin of Canadian Petroleum Geology 44, 244–257.

Srodon, J., 1980. Precise identification of illite/smectite interstratifica-

tions by powder X-ray diffraction. Clays and Clay Minerals 28, 401–411.

Tribble, J.S., 1990. Clay diagenesis in the Barbados accretionary complex: potential impact on hydrology and subduction dynamics. In: Moore, J.C., Mascle, A. (Eds.), Proceedings of the Ocean Drilling Program, Scientific Results 110, pp. 97–110.

van Moort, J.C., 1971. A comparative study of the diagenetic alteration of clay minerals in Mesozoic shales from Papua New Guinea and in Tertiary shales from Louisiana, U.S.A. Clays and Clay Minerals 19, 1–20.

Velde, B., 1985. Clay Minerals. A Physico-Chemical Explanation of Their Occurrence. Elsevier, Amsterdam.

Velde, B., Vasseur, G., 1992. Estimation of the diagenetic smectite-to-illite transformation in time–temperature space. American Mineralogist 77, 967–976.

Vrolijk, P., 1990. On the mechanical role of smectite in subduction zones. Geology 18, 703–707.

Wang, C.-Y., Mao, N.-H., 1979. Shearing of saturated clays in rock joints at high confining pressures. Geophysical Research Letters 6, 825–828.

Wang, C.-Y., Mao, N.-H., Wu, F.T., 1979. Mechanical properties of clay at high pressure. Journal of Geophysical Research 85, 1462–1468.

Weaver, C.E., Beck, K.C., 1971. Clay water diagenesis during burial: how mud becomes gneiss. Geological Society of America Special Paper 134.

Wilkens, R., McClellan, P., Moran, K., Tribble, J.S., Taylor, E., Verduzco, E., 1990. Diagenesis and dewatering of clay-rich sediments, Barbados accretionary prism. In: Moore, J.C., Mascle, A. (Eds.), Proceedings of the Ocean Drilling Program, Scientific Results 110, pp. 97–110.

Yeh, H.-S., Savin, S.M., 1977. The mechanism of burial diagenetic reactions in argillaceous sediments: 3. Oxygen isotope evidence. Geological Society of America Bulletin 88, 1321–1330.